

Advanced Quantizer Designs for FDD-based FD-MIMO Systems Using Uniform Planar Arrays

Jiho Song, *Student Member, IEEE*, Junil Choi, *Member, IEEE*, Taeyoung Kim, *Member, IEEE*, and David J. Love, *Fellow, IEEE*

Abstract—Massive multiple-input multiple-output (MIMO) systems, which utilize a large number of antennas at the base station, are expected to enhance network throughput by enabling improved multiuser MIMO techniques. To deploy many antennas in reasonable form factors, base stations are expected to employ antenna arrays in both horizontal and vertical dimensions, which is known as full-dimension (FD) MIMO. The most promising two-dimensional array is the uniform planar array (UPA), where antennas are placed in a grid pattern. To exploit the full benefit of massive MIMO in frequency division duplexing (FDD), the downlink channel state information (CSI) should be estimated, quantized, and fed back from the receiver to the transmitter. However, it is difficult to accurately quantize the channel in a computationally efficient manner due to the high dimensionality of the massive MIMO channel. In this paper, we develop both narrowband and wideband CSI quantizers for FD-MIMO taking the properties of realistic channels and the UPA into consideration. To improve quantization quality, we focus on not only quantizing dominant radio paths in the channel, but also combining the quantized beams. We also develop a hierarchical beam search approach, which scans both vertical and horizontal domains jointly with moderate computational complexity. Numerical simulations verify that the performance of the proposed quantizers is better than that of previous CSI quantization techniques.

Index Terms—Massive MIMO, full-dimension MIMO, uniform planar arrays, Kronecker product codebooks.

I. INTRODUCTION

MASSIVE multiple-input multiple-output (MIMO) systems are a strong candidate to fulfill the throughput requirements for fifth generation (5G) cellular networks [2]. To pack a sizable number of antennas in a limited area, uniform planar arrays (UPAs) that host antennas in both vertical and horizontal domains are being prominently considered in practice [3], [4]. Massive MIMO employing a UPA structure is known as full-dimension (FD) MIMO because of its ability to exploit both vertical and horizontal domain beamforming [5]–[10].

To fully exploit FD-MIMO, accurate channel state information (CSI) for both domains is critical. Channel estimation

techniques relying upon time division duplexing (TDD) can leverage channel reciprocity if the transmit and receive arrays are calibrated [11], [12]. Most current cellular systems, however, exploit frequency division duplexing (FDD) where the receiver should estimate, quantize, and feed back the downlink CSI to the transmitter. The high dimensionality of a massive MIMO channel could cause large overheads on downlink channel training and quantization processes [13]–[19]. We focus on CSI quantization for FD-MIMO in this paper and refer to [18]–[20] and the references therein for the massive MIMO downlink training problem.

The majority of CSI quantization codebooks have been designed under the assumption of spatially uncorrelated Rayleigh fading channels, which are uniformly distributed on the unit hypersphere when normalized. To quantize these channels, the codewords in a codebook should cover the unit sphere as uniformly as possible [21]–[23]. For spatially correlated channels, the codebooks have been carefully shaped based on the prior knowledge of channel statistics [24]–[28].

Although most previous codebooks have been designed based on analytical channel models, it is difficult to represent the properties of true three-dimensional (3D) channels for FD-MIMO. The 3D spatial channel model (SCM) in [4], [29], which is an extension of the 2D SCM [30], has been extensively used to mimic the measured channel variations for 3GPP standardization. Although the 3D SCM is a stochastic channel model, it provides limited insights into practical CSI quantizer designs. Therefore, it is necessary to develop a simple channel model that accurately represents the properties of the 3D-SCM channel with UPA antennas.

In this paper, we define a simple 3D channel model using the sum of a finite number of scaled array response vectors. Based on this simplified channel model, we develop CSI quantizers for UPA scenarios. We first carry out performance analysis of Kronecker product (KP) CSI quantizers [1], [9]. Our analytical studies on the KP CSI quantizers provide design guidelines on how to develop a quantizer for a narrowband, single frequency tone CSI using limited feedback resources. In the proposed quantizer, we concentrate on detecting/quantizing dominant radio paths in true channels. To maximize quantization quality, we also develop a codebook for combiners that cophases and scales the quantized beams. Both vertical and horizontal domains are exhaustively searched to locate beams properly, while this approach would involve a heavy computational complexity. We thus develop a hierarchical beam search approach to reduce the complexity.

We also develop a wideband quantizer for broadband

J. Song and D. J. Love are with the School of Electrical and Computer Engineering, Purdue University, West Lafayette, IN 47907 (e-mail: {jihosong, djlove}@purdue.edu).

J. Choi is with the Department of Electrical Engineering, POSTECH, Pohang, Gyeongbuk 37673, Korea (e-mail: junil@postech.ac.kr).

T. Kim, is with Samsung Electronics Co., Ltd., Suwon, Korea (email: ty33@samsung.com).

Parts of this paper were presented at the Globecom, Washington, DC USA, December 4-8, 2016 [1].

This work was supported in part by Communications Research Team (CRT), Samsung Electronics Co. Ltd., and the ICT R&D program of MSIP/IITP [2017(B0717-17-0002), Development of Integer-Forcing MIMO Transceivers for 5G & Beyond Mobile Communication Systems].

communication by evolving the dual codebook structure in LTE-Advanced [31], [32]. In the dual codebook structure, a first layer quantizer is used to search correlated CSI between multiple frequency tones. Unless dominant paths are gathered in a single cluster, the LTE-Advanced codebook is not effective because only adjacent radio paths are selected and quantized using the same resolution codebook. We thus concentrate on detecting adjacent and/or sperate paths within each wideband resource block (RB) based on the proposed hierarchical beam search approach. In addition, a second layer quantizer is designed to refine the beam direction of the quantized wideband CSI according to the channel vectors in a narrowband RB. When comparing our approach to the LTE-Advanced codebook, the refined beams are cophased and scaled in our approach, while the LTE-Advanced codebook only tries to cophase adjacent beams without considering beam refinement.

In Section II, we describe FD-MIMO systems employing UPAs and discuss a simple channel model that mimics true 3D SCM channels. In Section III, we review previously reported KP codebooks. In Section IV, we develop a narrowband CSI quantizer that takes multiple radio paths into account and conduct performance analysis to develop a design guideline for CSI quantizers. In Section V, we also propose a wideband CSI quantizer assuming a multi-carrier framework. In Section VI, we present simulation results, and the conclusion follows in Section VII.

Throughout this paper, \mathbb{C} denotes the field of complex numbers, \mathbb{N} denotes the semiring of natural numbers, $\mathcal{CN}(\mu, \sigma^2)$ denotes the complex normal distribution with mean μ and variance σ^2 , $[a, b]$ is the closed interval between a and b , $\mathcal{U}(a, b)$ denotes the uniform distribution in the closed interval $[a, b]$, $\lceil \cdot \rceil$ is the ceiling function, $\Gamma(n)$ denotes the complete gamma function, $\mathbb{E}_a[\cdot]$ is the expectation of independent random variables \mathbf{a} , $\|\cdot\|_p$ is the p -norm, \odot is the Hadamard product, \otimes is the Kronecker product, $\mathbf{0}_a$ is the $a \times 1$ all zeros vector, \mathbf{I}_N is the $N \times N$ identity matrix, $\mathbf{1}_{a,b}$ is the $a \times b$ all ones matrix, $\mathbf{A}_{a,b}$, $\mathbf{v}_{\max}\{\mathbf{A}\}$, and $\mathbf{eig}_{\max}\{\mathbf{A}\}$ denote $(a, b)^{th}$ entry, the principal eigenvector, and the principal eigenvalue of the matrix \mathbf{A} . Also, \mathbf{a}^H , \mathbf{a}^* , $(\mathbf{a})_\ell$, $\mathbf{a}_{[a:b]}$ denote the conjugate transpose, element-wise complex conjugate, ℓ -th entry, and subvector including entries between $[a, b]$ of the column vector \mathbf{a} , respectively.

II. SYSTEM MODEL

We consider multiple-input single-output (MISO) systems employing $M \doteq M_v M_h$ transmit antennas at the base station and a single receive antenna at the user, where M_v is the number of rows and M_h is the number of columns of the UPA antenna structure [3]. Assuming a multi-carrier framework, an input-output expression is defined as

$$y[w] = \sqrt{\rho} \mathbf{h}[w]^H \mathbf{f}[w] s[w] + n[w], \quad (1)$$

where $y[w]$ is the received baseband symbol, ρ is the signal-to-noise ratio (SNR), $\mathbf{h}[w] \in \mathbb{C}^M$ is the block fading MISO channel, $\mathbf{f}[w] \in \mathbb{C}^M$ is the unit norm transmit beamformer, $s[w] \in \mathbb{C}$ is the data symbol with the power constraint $\mathbb{E}[|s[w]|^2] \leq 1$, and $n[w] \sim \mathcal{CN}(0, 1)$ is the additive white

Gaussian noise. Note that $w \in \{1, \dots, W\}$ denotes each frequency tone in the multi-carrier framework.

To facilitate quantizer designs, we mimic the 3D-SCM and define a simplified channel model with a few radio paths according to

$$\mathbf{h}[w] \doteq \sum_{p=1}^P e^{-j2\pi(w - \frac{W-1}{2})\Delta t_p} \alpha_p \mathbf{d}_M(\psi_p^v, \psi_p^h, w), \quad (2)$$

while the true 3D-SCM is used to present numerical results in Section VI. In (2), P is the number of dominant paths, Δ is the subcarrier spacing, t_p is the excess tap delay of the p -th radio path, α_p is the channel gain of the p -th radio path, and $\mathbf{d}_M(\psi_p^v, \psi_p^h, w)$ is the p -th radio path at given angles (ψ_p^v, ψ_p^h) . In the UPA scenario, a radio path for the w -th frequency tone is represented as

$$\mathbf{d}_M(\psi^v, \psi^h, w) \doteq \mathbf{d}_{M_v}(\psi^v, w) \otimes \mathbf{d}_{M_h}(\psi^h, w) \quad (3)$$

where the array response vector $\mathbf{d}_{M_a}(\psi_a, w)$ is defined as

$$\mathbf{d}_{M_a}(\psi^a, w) \doteq \frac{1}{\sqrt{M_a}} [1, e^{j\frac{2\pi d_a}{\lambda[w]}\psi^a}, \dots, e^{j\frac{2\pi d_a}{\lambda[w]}(M_a-1)\psi^a}]^T, \quad (4)$$

for $a \in \{v, h\}$. In (4), $\psi^v = \sin \phi^v$ and $\psi^h = \sin \phi^h \cos \phi^v$ [33]. Note that d_a is the antennas spacing, ϕ^a is the angle for the array vector, and $\lambda[w]$ is the wavelength for the w -th frequency tone CSI

$$\lambda[w] \doteq \frac{\lambda_c}{1 + \frac{\Delta}{f_c}(w - \frac{W+1}{2})} \quad (5)$$

where f_c is the center frequency satisfying $c = f_c \lambda_c$ with the speed of light c . Without loss of generality, a narrowband representation of channels is defined by plugging¹ $w = \frac{W+1}{2}$ into (2)

$$\begin{aligned} \mathbf{h} &= \sum_{p=1}^P \mathbf{d}_M(\psi_p^v, \psi_p^h) \alpha_p \\ &= \mathbf{D} \mathbf{a} \end{aligned} \quad (6)$$

where $\mathbf{D} \doteq [\mathbf{d}_M(\psi_1^v, \psi_1^h), \dots, \mathbf{d}_M(\psi_P^v, \psi_P^h)] \in \mathbb{C}^{M \times P}$ is the set of radio paths and $\mathbf{a} \doteq [\alpha_1, \dots, \alpha_P]^T \in \mathbb{C}^P$ is the set of complex channel gains. In the narrowband assumption, w is dropped for simplicity. We assume that the beam directions are uniformly distributed in both vertical and horizontal domains such as $\psi_p^v, \psi_p^h \sim \mathcal{U}(-1, 1)$ and are independent of channel gains $\alpha_p \sim \mathcal{CN}(0, 1)$.

In the limited feedback beamforming approach, each user chooses a transmit beamformer among codewords in the codebook $\mathcal{F} \doteq \{\mathbf{f}_1, \dots, \mathbf{f}_{2B_T}\}$ such that

$$\mathbf{f} = \arg \max_{\tilde{\mathbf{f}} \in \mathcal{F}} |\mathbf{h}^H \tilde{\mathbf{f}}|^2,$$

where B_T denotes the total feedback overhead. Based on the assumption that both transmitter and receiver know the predefined codebook, the B_T -bit index of the selected beamformer is fed back to the transmitter over the feedback link.

¹We consider the $\frac{W+1}{2}$ -th subcarrier to ignore beam squinting effects [34].

The majority of channel quantization codebooks have been designed for spatially correlated and uncorrelated Rayleigh fading channels [21]–[28]. These analytical channel models rely upon rich scattering environments so that each radio path has a limited effect on channel characterization. Thus, most previous beamformer codebooks focus on covering the unit hypersphere as uniformly as possible without considering each radio path individually. However, the analytical channel models are much different than realistic channel models that assume only a few dominant scatterers. Thus, this line-packing codebook design approach may not be effective when the number of antennas is large. To accurately quantize high-dimensional massive MIMO channels, it is critical to tailor the codebook to the realistic channels consisting of a limited number of radio paths.

III. KRONECKER PRODUCT CODEBOOK REVIEW - SINGLE BEAM CASE

It is critical in the FDD massive MIMO systems to quantize and feedback information about the high-dimensional channels to the transmitter [13]–[19]. Thus, CSI quantization codebooks have been developed to tailor the feedback link with limited overhead to the massive MIMO channels [15]–[17]. Among various CSI quantization techniques, KP codebooks are of great interest to quantize the channels in a computationally efficient manner by considering the 2D antenna structure [9], [10]. Based on the channel model in (6), KP codebooks focus on quantizing a radio path with UPA structure [6]–[8].

Most KP codebooks are based on the assumption that the covariance matrix of the channels is approximated by the KP of covariance matrices of vertical and horizontal domains such that [35]

$$\mathbf{R}_h \doteq \mathbf{E}_h[\mathbf{h}\mathbf{h}^H] \\ \simeq \mathbf{R}^v \otimes \mathbf{R}^h.$$

Thus, a KP codebook is of the form

$$\mathcal{F} = \{\mathbf{f} \in \mathbb{C}^M : \mathbf{f} = \mathbf{c}^v \otimes (\mathbf{c}^h)^*, \mathbf{c}^v \in \mathcal{A}_{B_T/2}^v, \mathbf{c}^h \in \mathcal{A}_{B_T/2}^h\},$$

consider quantizing single dominant path with the discrete Fourier transform (DFT) codebook

$$\mathcal{A}_B^a = \{\mathbf{a}_{M_a}(1/Q), \dots, \mathbf{a}_{M_a}(Q/Q)\} \quad (7)$$

consisting of the $Q = 2^B$ codewords

$$\mathbf{a}_{M_a}(q/Q) \doteq \frac{1}{\sqrt{M_a}} \left[1, e^{j\pi(\frac{2q}{Q}-1)}, \dots, e^{j\pi(M_a-1)(\frac{2q}{Q}-1)} \right]^T.$$

Most previous KP codebooks quantize the first dominant vector in each domain separately [6]–[9]. To find singular vectors, the channel vector \mathbf{h} in (6) is decomposed into both vertical and horizontal domains based on the singular value decomposition [9] yielding

$$\mathbf{h} = \sum_{k=1}^{\text{rank}(\bar{\mathbf{H}})} (\mathbf{u}_k \otimes \mathbf{v}_k^*) \sigma_k, \quad (8)$$

where the reshaped channel is given in a matrix form

$$\bar{\mathbf{H}} \doteq [\mathbf{h}_{[1:M_h]}, \dots, \mathbf{h}_{[(M_v-1)M_h+1:M_v M_h]}]^T \in \mathbb{C}^{M_v \times M_h}.$$

In (8), σ_k denotes the k -th dominant singular value, $\mathbf{u}_k \in \mathbb{C}^{M_v}$ denotes the k -th dominant left singular vector, and $\mathbf{v}_k \in \mathbb{C}^{M_h}$ denotes the k -th dominant right singular vector of $\bar{\mathbf{H}}$. The final codeword is then obtained as $\mathbf{f} = \mathbf{c}^v \otimes (\mathbf{c}^h)^*$, where

$$\mathbf{c}^v = \arg \max_{\tilde{\mathbf{c}}^v \in \mathcal{A}_{B_T/2}^v} |\mathbf{u}_1^H \tilde{\mathbf{c}}^v|^2, \quad \mathbf{c}^h = \arg \max_{\tilde{\mathbf{c}}^h \in \mathcal{A}_{B_T/2}^h} |\mathbf{v}_1^H \tilde{\mathbf{c}}^h|^2.$$

Despite the advantage of a KP codebook, it has some issues. Even with a line-of-sight (LOS) channel, a dominant radio path may not be accurately quantized by searching each domain separately. Also, it is not always effective to quantize only a single radio path because even $\mathbf{u}_1 \otimes \mathbf{v}_1^*$ may consist of multiple paths. Although the quantizer in [9] considers adding two beams in $\mathbf{u}_1 \otimes \mathbf{v}_1^*$, the performance improvement is limited because the beams are not combined properly.

IV. PROPOSED NARROWBAND QUANTIZER - MULTIPLE BEAMS CASE

Prior work has verified that most 3D SCM channel realizations are well modeled with only a few resolvable 2D radio paths [1], [9]. Thus, we assume that the channel vector on a single frequency tone can be represented by a combination of a set of multiple radio paths and its corresponding channel gain vector [1]. In (6), the array response vectors in \mathbf{D} and the channel gain vector \mathbf{a} contain different types of channel information. Thus, we focus on quantizing \mathbf{D} and \mathbf{a} using different codebooks in this paper.

In our narrowband quantizer, we aim to find

$$\mathbf{h}/\|\mathbf{h}\|_2 \simeq \mathbf{C}\mathbf{z}/\|\mathbf{C}\mathbf{z}\|_2 \quad (9)$$

by constructing a set of N beams $\mathbf{C} \doteq [\mathbf{c}_1, \dots, \mathbf{c}_N] \in \mathbb{C}^{M \times N}$ and an unit norm weight vector $\mathbf{z} \doteq [z_1, \dots, z_N]^T \in \mathbb{C}^N$. The radio paths constituting the channels are represented by the Kronecker product of array response vectors as in (3). Thus, each 2D beam in \mathbf{C} can be defined by a combination of quantized array response vectors in vertical and horizontal domains such that

$$\mathbf{c}_n \doteq \mathbf{c}_n^v \otimes \mathbf{c}_n^h, \quad n = 1, \dots, N.$$

We assume that B_n -bit is reserved to quantize the n -th array response vector \mathbf{c}_n^a in the domain a and B_c -bit is reserved to quantize the weight vector \mathbf{z} .

To construct \mathbf{C} and \mathbf{z} under the condition of a limited feedback overhead of $B_T = B_c + \sum_{n=1}^N 2B_n$ -bits, the following questions should be properly addressed.

- 1) **Beam quantization:** How should the radio paths in the channel be chosen and quantized?
- 2) **Beam combining:** How should the quantized beams be cophased and scaled?
- 3) **Feedback resource allocation:** For a given total feedback overhead B_T , how should the feedback-bit allocation scenario

$$\mathbf{r}_N \doteq [B_1, \dots, B_N, B_c]^T \in \mathbb{N}^{N+1} \quad (10)$$

be defined to effectively quantize and combine the limited number of radio paths?

In the following subsections, we address our channel quantization procedure across two separate quantization phases and evaluate quantization loss at each phase.

Remark 1: The quantized channel vector can be viewed as a representation of the channel using an analog beamsteering matrix \mathbf{C} , which is realized by a set of radio frequency phase shifters, and a baseband beamformer \mathbf{z} . Therefore, the proposed approach follows the hybrid beamforming architecture in [36].

A. Phase I: Beam Quantization

In the beam quantization phase, we aim to construct a selected set of quantized 2D beams \mathbf{C} . It is well known that the DFT codebook is an effective solution to quantize array response vectors so that we quantize the n -th array response vector \mathbf{c}_n^a with the DFT codebook $\mathcal{A}_{B_n}^a$.

In our beam quantization approach, we choose and quantize each 2D DFT beam one-by-one as well as update the weight vector iteratively. In the n -th update, the quantized DFT vectors and the unquantized weight vector² are obtained by solving the maximization problem

$$(\mathbf{c}_n^v, \mathbf{c}_n^h, \bar{\mathbf{z}}_n) = \arg \max_{(\tilde{\mathbf{c}}^v, \tilde{\mathbf{c}}^h, \tilde{\mathbf{z}}) \in \mathcal{A}_{B_n}^v \times \mathcal{A}_{B_n}^h \times \mathbb{C}^n} \frac{|\mathbf{h}^H \mathbf{C}_{n|\tilde{\mathbf{c}}^v, \tilde{\mathbf{c}}^h} \tilde{\mathbf{z}}|^2}{\|\mathbf{C}_{n|\tilde{\mathbf{c}}^v, \tilde{\mathbf{c}}^h} \tilde{\mathbf{z}}\|_2^2}, \quad (11)$$

where $\mathbf{C}_{n|\tilde{\mathbf{c}}^v, \tilde{\mathbf{c}}^h} \doteq [\mathbf{c}_1, \dots, \mathbf{c}_{n-1}, \tilde{\mathbf{c}}^v \otimes \tilde{\mathbf{c}}^h] \in \mathbb{C}^{M \times n}$, and $\{\mathbf{c}_1, \dots, \mathbf{c}_{n-1}\}$ includes previously selected DFT beams.

In (11), we do not quantize the weight vector $\bar{\mathbf{z}}_n \in \mathbb{C}^n$ because it is not practical to construct a codebook for weight vectors that constantly change its dimension in each update. For a given $\tilde{\mathbf{c}}^v$ and $\tilde{\mathbf{c}}^h$, the unquantized weight vector is thus computed based on the generalized Rayleigh quotient as [37]

$$\begin{aligned} \bar{\mathbf{z}}_{n|\tilde{\mathbf{c}}^v, \tilde{\mathbf{c}}^h} &= \arg \max_{\tilde{\mathbf{z}} \in \mathbb{C}^n} \frac{\tilde{\mathbf{z}}^H (\mathbf{C}_{n|\tilde{\mathbf{c}}^v, \tilde{\mathbf{c}}^h}^H \mathbf{h} \mathbf{h}^H \mathbf{C}_{n|\tilde{\mathbf{c}}^v, \tilde{\mathbf{c}}^h}) \tilde{\mathbf{z}}}{\tilde{\mathbf{z}}^H (\mathbf{C}_{n|\tilde{\mathbf{c}}^v, \tilde{\mathbf{c}}^h}^H \mathbf{C}_{n|\tilde{\mathbf{c}}^v, \tilde{\mathbf{c}}^h}) \tilde{\mathbf{z}}} \\ &= \mathbf{v}_{\max} \{ (\mathbf{C}_{n|\tilde{\mathbf{c}}^v, \tilde{\mathbf{c}}^h}^H \mathbf{C}_{n|\tilde{\mathbf{c}}^v, \tilde{\mathbf{c}}^h})^{-1} \mathbf{C}_{n|\tilde{\mathbf{c}}^v, \tilde{\mathbf{c}}^h}^H \mathbf{h} \mathbf{h}^H \mathbf{C}_{n|\tilde{\mathbf{c}}^v, \tilde{\mathbf{c}}^h} \}. \end{aligned}$$

By plugging the weight vector into the maximizer, the problem of choosing the n -th 2D DFT beam is simplified as

$$(\mathbf{c}_n^v, \mathbf{c}_n^h) = \arg \max_{(\tilde{\mathbf{c}}^v, \tilde{\mathbf{c}}^h) \in \mathcal{A}_{B_n}^v \times \mathcal{A}_{B_n}^h} \frac{|\mathbf{h}^H \mathbf{C}_{n|\tilde{\mathbf{c}}^v, \tilde{\mathbf{c}}^h} \bar{\mathbf{z}}_{n|\tilde{\mathbf{c}}^v, \tilde{\mathbf{c}}^h}|^2}{\|\mathbf{C}_{n|\tilde{\mathbf{c}}^v, \tilde{\mathbf{c}}^h} \bar{\mathbf{z}}_{n|\tilde{\mathbf{c}}^v, \tilde{\mathbf{c}}^h}\|_2^2}.$$

This beam quantization algorithm is summarized in Algorithm 1. The iterative approach gives a set of N quantized beams

$$\mathbf{C} = [\mathbf{c}_1, \dots, \mathbf{c}_N] \in \mathbb{C}^{M \times N} \quad (12)$$

and the unquantized weight vector

$$\bar{\mathbf{z}} = \bar{\mathbf{z}}_{N|\mathbf{c}_N^v, \mathbf{c}_N^h} \in \mathbb{C}^N. \quad (13)$$

We also evaluate quantization loss due to the beam quantization as a function of the number of beams N and the feedback overhead B_n for DFT codebooks. Assuming the unquantized weight vector $\bar{\mathbf{z}}$, the beamforming gain between the channel vector \mathbf{h} and the set of DFT beams \mathbf{C}

$$\begin{aligned} G^{\text{bq}} &\doteq \mathbb{E}_{\mathbf{h}} [\mathbf{h}^H \mathbf{C} \bar{\mathbf{z}} / \|\mathbf{C} \bar{\mathbf{z}}\|_2^2] \\ &= \mathbb{E}_{\mathbf{h}} \left[\max_{\tilde{\mathbf{z}} \in \mathbb{C}^N} \frac{|\mathbf{h}^H \mathbf{C} \tilde{\mathbf{z}}|^2}{\|\mathbf{C} \tilde{\mathbf{z}}\|_2^2} \right] \end{aligned} \quad (14)$$

²The bar on the top of weight vectors denotes that the weight vectors are not quantized.

Algorithm 1 Beam quantization

Initialization

1: Create an initial empty matrix \mathbf{C}_0

Iterative update

2: **for** $1 \leq n \leq N$

3: Quantize radio path $\mathbf{c}_n = \mathbf{c}_n^v \otimes \mathbf{c}_n^h \in \mathbb{C}^M$

4: Update weight vector $\bar{\mathbf{z}}_n = \bar{\mathbf{z}}_{n|\mathbf{c}_n^v, \mathbf{c}_n^h} \in \mathbb{C}^n$ where

5: $(\mathbf{c}_n^v, \mathbf{c}_n^h) = \arg \max_{\tilde{\mathbf{c}}^v, \tilde{\mathbf{c}}^h \in \mathcal{A}_{B_n}^v \times \mathcal{A}_{B_n}^h} \frac{|\mathbf{h}^H \mathbf{C}_{n|\tilde{\mathbf{c}}^v, \tilde{\mathbf{c}}^h} \bar{\mathbf{z}}_{n|\tilde{\mathbf{c}}^v, \tilde{\mathbf{c}}^h}|^2}{\|\mathbf{C}_{n|\tilde{\mathbf{c}}^v, \tilde{\mathbf{c}}^h} \bar{\mathbf{z}}_{n|\tilde{\mathbf{c}}^v, \tilde{\mathbf{c}}^h}\|_2^2}$

6: $\mathbf{C}_{n|\tilde{\mathbf{c}}^v, \tilde{\mathbf{c}}^h} \doteq [\mathbf{c}_1, \dots, \mathbf{c}_{n-1}, \tilde{\mathbf{c}}^v \otimes \tilde{\mathbf{c}}^h] \in \mathbb{C}^{M \times n}$

7: $\bar{\mathbf{z}}_{n|\tilde{\mathbf{c}}^v, \tilde{\mathbf{c}}^h} =$

$$\mathbf{v}_{\max} \{ (\mathbf{C}_{n|\tilde{\mathbf{c}}^v, \tilde{\mathbf{c}}^h}^H \mathbf{C}_{n|\tilde{\mathbf{c}}^v, \tilde{\mathbf{c}}^h})^{-1} \mathbf{C}_{n|\tilde{\mathbf{c}}^v, \tilde{\mathbf{c}}^h}^H \mathbf{h} \mathbf{h}^H \mathbf{C}_{n|\tilde{\mathbf{c}}^v, \tilde{\mathbf{c}}^h} \}$$

8: **end for**

Final update

9: Quantized radio paths $\mathbf{C} = [\mathbf{c}_1, \dots, \mathbf{c}_N] \in \mathbb{C}^{M \times N}$

10: Unquantized weight vector $\bar{\mathbf{z}} = \bar{\mathbf{z}}_{N|\mathbf{c}_N^v, \mathbf{c}_N^h} \in \mathbb{C}^N$

is averaged over channel realizations \mathbf{h} in Lemma 1. Before presenting the lemma, we made the following assumption.

Assumption 1: Assuming a channel vector \mathbf{h} has already been decomposed into a set of radio paths \mathbf{D} and channel gains \mathbf{a} as in (6), the column vectors for each domain $a \in \{h, v\}$ in \mathbf{C} are separately selected as $\mathbf{c}_n^a \doteq \mathbf{a}_{M_a}(q_n/2^{B_n}) \in \mathcal{A}_{B_n}^a$, where

$$q_n = \arg \max_{q \in \{1, \dots, 2^{B_n}\}} |\mathbf{d}_{M_a}^H(\psi_n^a) \mathbf{a}_{M_a}(q/2^{B_n})|^2. \quad (15)$$

Considering half-wavelength antenna spacing $d_a = \frac{\lambda}{2}$, the beamforming gain between the n -th array response vector and the selected DFT vector $\Gamma_{na}^2 \doteq \mathbb{E}[|\mathbf{d}_{M_a}^H(\psi_n^a) \mathbf{c}_n^a|^2]$ is derived in Appendix A as

$$\Gamma_{na}^2 = \frac{1}{M_a^2} \left(M_a + \sum_{q=1}^{M_a-1} \frac{2(M_a - q) \sin(\pi q/2^{B_n})}{\pi q/2^{B_n}} \right).$$

Lemma 1: A lower bound of the beamforming gain G^{bq} in (14) is approximated as

$$G^{\text{bq}} \simeq \frac{P}{M + N - 1} \left(N + \sum_{n=1}^N \sum_{q=n}^P \frac{M \Gamma_{nv}^2 \Gamma_{nh}^2 - 1}{qP} \right).$$

Please check Appendix B for the proof.

B. Phase II: Beam Combining

In the beam combining phase, we aim to compute a weight vector \mathbf{z} , which is used to combine beams in \mathbf{C} . To quantize weight vector

$$\mathbf{z} = \arg \max_{\tilde{\mathbf{z}} \in \mathcal{Z}_{B_c}} \frac{|\mathbf{h}^H \mathbf{C} \tilde{\mathbf{z}}|^2}{\|\mathbf{C} \tilde{\mathbf{z}}\|_2^2}, \quad (16)$$

we design the codebook including $U = 2^{B_c}$ unit norm combiners $\mathcal{Z}_{B_c} \doteq \{\mathbf{z}_1, \dots, \mathbf{z}_U\}$. To study a codebook design framework, we model the effective channel vector based on the Kronecker correlation model as

$$\mathbf{C}^H \mathbf{h} \simeq \mathbf{R}^{\frac{1}{2}} \mathbf{w} \in \mathbb{C}^N, \quad (17)$$

$$\mathbf{R} = \begin{bmatrix} \mathbf{E}_h[(\mathbf{c}_1^v \otimes \mathbf{c}_1^h)^H \mathbf{h} \mathbf{h}^H (\mathbf{c}_1^v \otimes \mathbf{c}_1^h)] & \cdots & \mathbf{E}_h[(\mathbf{c}_1^v \otimes \mathbf{c}_1^h)^H \mathbf{h} \mathbf{h}^H (\mathbf{c}_N^v \otimes \mathbf{c}_N^h)] \\ \vdots & \ddots & \vdots \\ \mathbf{E}_h[(\mathbf{c}_N^v \otimes \mathbf{c}_N^h)^H \mathbf{h} \mathbf{h}^H (\mathbf{c}_1^v \otimes \mathbf{c}_1^h)] & \cdots & \mathbf{E}_h[(\mathbf{c}_N^v \otimes \mathbf{c}_N^h)^H \mathbf{h} \mathbf{h}^H (\mathbf{c}_N^v \otimes \mathbf{c}_N^h)] \end{bmatrix}. \quad (18)$$

where the covariance matrix $\mathbf{R} \doteq \mathbf{E}_h[\mathbf{C}^H \mathbf{h} \mathbf{h}^H \mathbf{C}] \in \mathbb{C}^{N \times N}$ in (18) is analytically computed in Appendix C and random variables $\mathbf{w} = [w_1, \dots, w_N]^T \in \mathcal{W}$ denotes the weight vector that is subject to the equal gain subset

$$\mathcal{W} \doteq \{\mathbf{w} \in \mathbb{C}^N : w_n = e^{j\vartheta_n} / \sqrt{N}, \vartheta_n \sim \mathcal{U}(0, 2\pi)\}.$$

In our codebook design approach, we pick a set of codewords $\{\mathbf{z}_1 \cdots \mathbf{z}_U\}$ that maximize

$$\begin{aligned} \sigma_{\min} &= \min_{1 \leq u \leq U} \frac{|\mathbf{h}^H \mathbf{C} \mathbf{z}_u|^2}{\|\mathbf{C} \mathbf{z}_u\|_2^2} \\ &\stackrel{(a)}{\geq} \min_{1 \leq u \leq U} \frac{|\mathbf{h}^H \mathbf{C} \mathbf{z}_u|^2}{\|\mathbf{C}\|_2^2} \\ &\stackrel{(b)}{\simeq} \min_{1 \leq u \leq U} \frac{|\mathbf{w}^H (\mathbf{R}^{\frac{1}{2}})^H \mathbf{z}_u|^2}{\|\mathbf{C}\|_2^2}, \end{aligned}$$

where the inequality in (a) is based on $\|\mathbf{C} \mathbf{z}_u\|_2^2 \leq \|\mathbf{C}\|_2^2 \|\mathbf{z}_u\|_2^2$ and $\|\mathbf{z}_u\|_2^2 = 1$, and (b) is approximated by plugging the Kronecker correlation model in (17) into the maximizer.

Based on the *correlated Grassmannian beamforming* algorithm in [24], codewords are then obtained by setting

$$\mathbf{z}_u = \mathbf{R}^{\frac{1}{2}} \mathbf{e}_u / \|\mathbf{R}^{\frac{1}{2}} \mathbf{e}_u\|_2$$

and picking a set of equal gain vectors $\{\mathbf{e}_1 \cdots \mathbf{e}_U\}$ maximizing

$$\varrho_{\min} = \min_{1 \leq a < b \leq U} \sqrt{1 - |\mathbf{e}_a^H \mathbf{e}_b|^2},$$

where equal gain vectors $\mathbf{e}_u \in \mathcal{E}_N$ are restricted to

$$\mathcal{E}_N \doteq \{\mathbf{e} \in \mathbb{C}^N : (\mathbf{e})_n = e^{j2\pi\varphi_n} / \sqrt{N}, \varphi_n \in \{1/I \cdots I/I\}\}.$$

Note that $I \in \mathbb{N}$ denotes the phase quantization level.

We also evaluate the quantization loss due to the beam combining as a function of the number of codewords $U = 2^{B_c}$ in the codebook \mathcal{Z}_{B_c} that quantizes the baseband combiner $\bar{\mathbf{z}}$ in (13). To analyze quantization performance of \mathcal{Z}_{B_c} , the normalized beamforming gain between the normalized effective channel and the selected unit norm combiner \mathbf{z}

$$\begin{aligned} G^{\text{bc}} &\doteq \mathbf{E}_{\mathbf{h}^H \mathbf{C}} [|\mathbf{h}^H \mathbf{C} \mathbf{z}|^2 / \|\mathbf{h}^H \mathbf{C}\|_2^2] \\ &\simeq \mathbf{E}_{\mathbf{w}} \left[\max_{u \in \{1, \dots, U\}} \frac{|\mathbf{e}_u^H \mathbf{R} \mathbf{w}|^2}{(\mathbf{w}^H \mathbf{R} \mathbf{w})(\mathbf{e}_u^H \mathbf{R} \mathbf{e}_u)} \right] \end{aligned} \quad (19)$$

is averaged over the effective channel $\mathbf{C}^H \mathbf{h}$. Because it is not easy to compute in a closed form, we only derive the normalized beamforming gain in the special case of $N = 2$ based on the following assumption.

Assumption 2: For simple analysis, we assume that the combiner is selected as $\mathbf{z} \doteq \mathbf{z}_{\hat{u}}$, where

$$\hat{u} \doteq \arg \max_{u \in \{1, \dots, U\}} \cos^2 \theta_u.$$

Note that $\theta_u \doteq \arccos |\mathbf{w}^H \mathbf{e}_u|$.

Lemma 2: In the special case of $N = 2$, the normalized beamforming gain G^{bc} in (19) is approximated as

$$G^{\text{bc}} \simeq \frac{1}{2} \left(1 + \frac{2^{B_c}}{\pi} \sin \frac{\pi}{2^{B_c}} \right).$$

Please check Appendix D for the proof.

C. Feedback Resource Allocation

In our KP codebook procedure, quantizing more beams with a high resolution codebook increases the beamforming gain at the cost of increased feedback overhead. To effectively allocate limited feedback overhead resources, we must derive the beamforming gain between the randomly generated channel vectors \mathbf{h} and the selected codeword $\mathbf{C} \mathbf{z} / \|\mathbf{C} \mathbf{z}\|_2$ using

$$G \doteq \mathbf{E}_h [|\mathbf{h}^H \mathbf{C} \mathbf{z}|^2 / \|\mathbf{C} \mathbf{z}\|_2^2] \quad (20)$$

as a function of the feedback-bit allocation scenario³ \mathbf{r}_N in (10). However, inter-dependencies across both quantization phases in Section IV-A and Section IV-B make it hard to compute the beamforming gain in a closed form. To simplify analysis, we made the following assumption.

Assumption 3: Assuming the quantization phases in Section IV-A and Section IV-B work independently, the channel quantization quality in the proposed KP codebook procedure is evaluated by the combination of the quantization losses in both phases.

Based on Assumption 3 that both quantization phases are independent of each other, the beamforming gain in the proposed quantizer is defined by the mixture of G^{bq} and G^{bc} such as,

$$\begin{aligned} G(M, P, N, \mathbf{r}_N) &\doteq G^{\text{bq}} G^{\text{bc}} \\ &= \frac{G^{\text{bc}} (PN + \sum_{n=1}^N \sum_{q=n}^P \frac{M \Gamma_{nv}^2 \Gamma_{nh}^2 - 1}{q})}{M + N - 1}, \end{aligned} \quad (21)$$

where M is the number of antennas, P is the number of beams in \mathbf{h} , N is the number of dominant beams to be quantized, and \mathbf{r}_N is the feedback-bit allocation scenario in (10).

In the proposed quantizer, the feedback scenario are chosen as

$$(N, \mathbf{r}_N) = \arg \max_{(\tilde{N}, \tilde{\mathbf{r}}_{\tilde{N}}) \in \mathcal{N} \times \mathbb{N}^{\tilde{N}+1}} \mathbf{E}_P [G(M, P, \tilde{N}, \tilde{\mathbf{r}}_{\tilde{N}})] \quad (22)$$

by evaluating all possible scenarios $\tilde{\mathbf{r}}_{\tilde{N}} = [\tilde{B}_1, \dots, \tilde{B}_{\tilde{N}}, \tilde{B}_c]^T$ that considers \tilde{N} beams in $\mathcal{N} \doteq \{1, 2, 3\}$. Note that the possible feedback scenarios are subject to the total feedback overhead $B_T = \tilde{B}_c + \sum_{n=1}^{\tilde{N}} 2\tilde{B}_n$ -bits. In (22), the expectation is taken over the number of dominant paths P since P varies

³In \mathbf{r}_N , B_n for $n \in \{1, \dots, N\}$ denotes the size in bits of the DFT codebooks $\mathcal{A}_{B_n}^a$ in the domain a , and B_c denotes the size in bits of the codebook for combiners \mathcal{Z}_{B_c} .

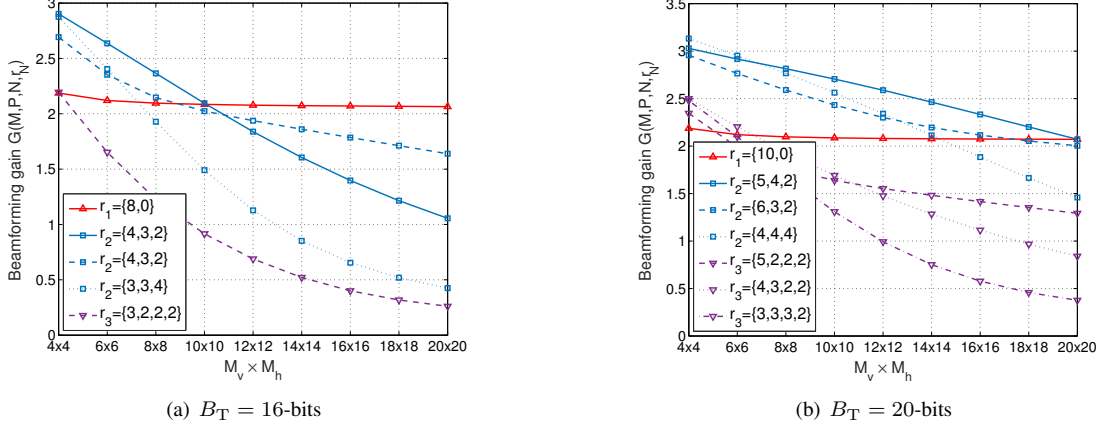


Fig. 1. Cross correlation $G(M, P, N, \mathbf{r}_N)$ over different feedback-bit allocation scenarios with $P \in \{3, 4, 5\}$.

depending on the channel environments. By assuming P is equally probable from 3 to 5, we plot the arithmetic mean of $G(M, P, \tilde{N}, \mathbf{r}_{\tilde{N}})$ in Fig. 1 with different numbers of antennas and feedback bits.

As shown in the figure, quantizing one or two beams give the best performance under practical UPA scenarios and feedback overheads. Therefore, we construct the codebook \mathcal{F}_1 for quantizing a single 2D DFT beam and the codebook \mathcal{F}_2 combining two quantized 2D DFT beams based on the predefined feedback-bit allocation scenarios⁴

$$\mathbf{r}_1 = [B_1 + \tilde{B}_1, 0] \in \mathbb{N}^2, \quad \mathbf{r}_2 = [B_1, B_2, B_c] \in \mathbb{N}^3, \quad (23)$$

respectively. The final codebook is then defined such that

$$\mathcal{F} \doteq \mathcal{F}_1 \cup \mathcal{F}_2.$$

D. Beam Search Approach

It is necessary to search both vertical and horizontal domains jointly to scan for the dominant beams in a channel vector. However, this joint approach increases a computational complexity. For example, it is required to carry out $2^{2(B_1 + \tilde{B}_1)}$ vector computations to scan a single 2D DFT beam under the feedback-bit allocation scenario \mathbf{r}_1 in (23). To reduce the heavy computational complexity that comes with detecting the single dominant beam, we propose a multi-round beam search technique as follows.

Round 1: For the channel vector \mathbf{h} , the first dominant beam is chosen using DFT codebooks $\mathcal{A}_{B_1}^v$ and $\mathcal{A}_{B_1}^h$ in (7), which have low-resolution DFT vectors. The DFT beam is given by

$$\begin{aligned} \mathbf{c}_1 &= \mathbf{c}_1^v \otimes \mathbf{c}_1^h, \\ (\mathbf{c}_1^v, \mathbf{c}_1^h) &= \arg \max_{(\tilde{\mathbf{c}}^v, \tilde{\mathbf{c}}^h) \in \mathcal{A}_{B_1}^v \times \mathcal{A}_{B_1}^h} |\mathbf{h}^H(\tilde{\mathbf{c}}^v \otimes \tilde{\mathbf{c}}^h)|^2. \end{aligned} \quad (24)$$

Later, the selected 2D DFT beam in (24) will be a baseline that guides the generation of two codeword candidates.

Round 2: In this round, $2\tilde{B}_1$ -bits are assigned for constructing the two codeword candidates.

⁴The total feedback overhead for feedback scenarios are $B_T = 2B_1 + 2\tilde{B}_1$ -bits and $B_T = 2B_1 + 2B_2 + B_c$ -bits, where $2\tilde{B}_1 = 2B_2 + B_c$.

1) To support channel realizations having a single dominant beam, a codeword is computed based on the feedback-bit allocation scenario \mathbf{r}_1 in (23) by scanning beam directions near \mathbf{c}_1 from Round 1. The first codeword is given by

$$\begin{aligned} \mathbf{f}_1 &= \check{\mathbf{d}}_M(\theta_1^v, \theta_1^h) \odot \mathbf{c}_1, \\ (\theta_1^v, \theta_1^h) &= \arg \max_{\tilde{\theta}^v, \tilde{\theta}^h \in \mathcal{T}_{B_1}^{\tilde{B}_1}} |\mathbf{h}^H(\check{\mathbf{d}}_M(\tilde{\theta}^v, \tilde{\theta}^h) \odot \mathbf{c}_1)|^2 \end{aligned}$$

where $\check{\mathbf{d}}_M(\theta^v, \theta^h) \doteq \sqrt{M} \mathbf{d}_M(\theta^v, \theta^h)$ is defined to shift the beam directions⁵ and the \tilde{B}_1 -bit size codebook

$$\mathcal{T}_{B_1}^{\tilde{B}_1} = \left\{ -\frac{1-2^{-\tilde{B}_1}}{2^{B_1+1}} : 2^{-(B_1+\tilde{B}_1)} : \frac{1-2^{-\tilde{B}_1}}{2^{B_1+1}} \right\} \quad (25)$$

is designed for refining beam directions of any DFT beams.

In our CSI quantization approach, the first codebook is then defined such that

$$\mathcal{F}_1 \doteq \{\mathbf{f}_1 \in \mathbb{C}^M : \mathbf{f}_1 = (\tilde{\mathbf{c}}_1^v \otimes \tilde{\mathbf{c}}_1^h) \odot \check{\mathbf{d}}_M(\tilde{\theta}^v, \tilde{\theta}^h)\}$$

over $\tilde{\mathbf{c}}_1^v \in \mathcal{A}_{B_1}^v$, $\tilde{\mathbf{c}}_1^h \in \mathcal{A}_{B_1}^h$, and $\tilde{\theta}^v, \tilde{\theta}^h \in \mathcal{T}_{B_1}^{\tilde{B}_1}$.

2) To support channel realizations having multiple dominant beams, a codeword is computed based on the feedback-bit allocation scenario \mathbf{r}_2 in (23) by choosing an additional DFT beam to combine with \mathbf{c}_1 . The second codeword is given by

$$\mathbf{f}_2 = \frac{[\mathbf{c}_1, \mathbf{c}_2^v \otimes \mathbf{c}_2^h] \mathbf{z}}{\|[\mathbf{c}_1, \mathbf{c}_2^v \otimes \mathbf{c}_2^h] \mathbf{z}\|_2},$$

$$(\mathbf{c}_2^v, \mathbf{c}_2^h, \mathbf{z}) = \arg \max_{(\tilde{\mathbf{c}}^v, \tilde{\mathbf{c}}^h, \tilde{\mathbf{z}}) \in \mathcal{A}_{B_2}^v \times \mathcal{A}_{B_2}^h \times \mathcal{Z}_{B_c}} \left| \frac{\mathbf{h}^H[\mathbf{c}_1, \tilde{\mathbf{c}}^v \otimes \tilde{\mathbf{c}}^h] \tilde{\mathbf{z}}}{\|[\mathbf{c}_1, \tilde{\mathbf{c}}^v \otimes \tilde{\mathbf{c}}^h] \tilde{\mathbf{z}}\|_2} \right|^2$$

using B_2 -bits size DFT codebooks $\mathcal{A}_{B_2}^v$ and $\mathcal{A}_{B_2}^h$ and B_c -bits size codebook \mathcal{Z}_{B_c} , which is developed to combine the two 2D DFT beams as explained in the Section IV-B.

Considering our CSI quantization technique, the second codebook is then defined such that

$$\mathcal{F}_2 \doteq \left\{ \mathbf{f}_2 \in \mathbb{C}^M : \mathbf{f}_2 = \frac{[\tilde{\mathbf{c}}_1^v \otimes \tilde{\mathbf{c}}_1^h, \tilde{\mathbf{c}}_2^v \otimes \tilde{\mathbf{c}}_2^h] \tilde{\mathbf{z}}}{\|[\tilde{\mathbf{c}}_1^v \otimes \tilde{\mathbf{c}}_1^h, \tilde{\mathbf{c}}_2^v \otimes \tilde{\mathbf{c}}_2^h] \tilde{\mathbf{z}}\|_2} \right\}$$

⁵The Hadamard product formulation satisfies the following formulation $\sqrt{M} \mathbf{d}_M(\theta_1, \theta_3) \odot \mathbf{d}_M(\theta_2, \theta_4) = \mathbf{d}_M(\theta_1 + \theta_2, \theta_3 + \theta_4)$.

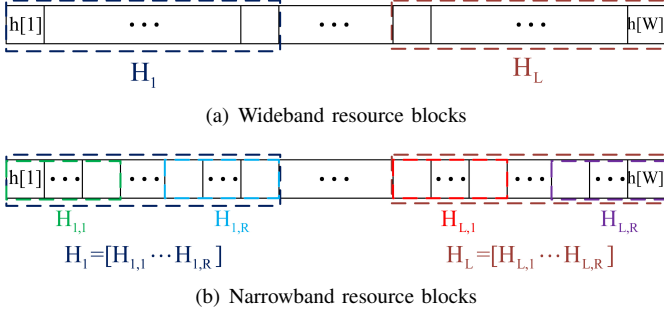


Fig. 2. An overview of wideband model having multiple tones.

over $\tilde{\mathbf{c}}_1^v \in \mathcal{A}_{B_1}^v$, $\tilde{\mathbf{c}}_1^h \in \mathcal{A}_{B_1}^h$, $\tilde{\mathbf{c}}_2^v \in \mathcal{A}_{B_2}^v$, $\tilde{\mathbf{c}}_2^h \in \mathcal{A}_{B_2}^h$, and $\tilde{\mathbf{z}} \in \mathcal{Z}_{B_c}$.

Round 3: Using the two codeword candidates $\mathbf{f}_1 \in \mathcal{F}_1$ and $\mathbf{f}_2 \in \mathcal{F}_2$, the final codeword is selected with an additional bit

$$\mathbf{f} = \arg \max_{\tilde{\mathbf{f}} \in \{\mathbf{f}_1, \mathbf{f}_2\}} |\mathbf{h}^H \tilde{\mathbf{f}}|^2. \quad (26)$$

V. PROPOSED WIDEBAND QUANTIZER

We develop a wideband quantizer that takes multiple frequency tones into account. Before developing practical quantizers, we overview a broadband system model adopted in 3GPP LTE-Advanced. As shown in Fig. 2(a), W total frequency tones are divided into L wideband RBs where each wideband RB includes $\frac{W}{L}$ channels. Each wideband RB is written in a matrix form as

$$\mathbf{H}_\ell = [\mathbf{h}[1 + (\ell - 1)W/L], \dots, \mathbf{h}[\ell W/L]] \in \mathbb{C}^{M \times \frac{W}{L}}.$$

As depicted in Fig. 2(b), each wideband RB is divided into R narrowband RBs

$$\mathbf{H}_\ell = [\mathbf{H}_{\ell,1}, \dots, \mathbf{H}_{\ell,R}],$$

where $\mathbf{H}_{\ell,r} \in \mathbb{C}^{M \times \frac{W}{LR}}$ denotes the narrowband RB that is written in a matrix form.

Next, the correlation between the channel vectors is studied numerically based on the cross correlations over $w_1 \neq w_2$

$$\gamma_{\mathbf{h}} \doteq \mathbb{E}_{\mathbf{h}[w]} \left[\frac{|\mathbf{h}[w_1]^H \mathbf{h}[w_2]|^2}{\|\mathbf{h}[w_1]\|_2^2 \|\mathbf{h}[w_2]\|_2^2} \right],$$

$$\gamma_{\mathbf{c}_1} \doteq \mathbb{E}_{\mathbf{c}_1[w]} \left[|\mathbf{c}_1[w_1]^H \mathbf{c}_1[w_2]|^2 \right],$$

where $\mathbf{h}[w]$ denotes 3D-SCM channel vectors and $\mathbf{c}_1[w]$ denotes the dominant 2D DFT beam that is chosen from the DFT codebooks \mathcal{A}_B^v and \mathcal{A}_B^h in (7) for subcarrier w . As shown in Fig. 3, it is verified that the dominant 2D DFT beams in the different subcarriers' channel vectors are highly correlated. Based on empirical studies, the wideband quantizer is designed in such a way that the correlated information, i.e., the dominant 2D DFT beam, is shared between neighboring subcarriers.

Level 1 (Wideband resource block): We choose two 2D DFT beams that are close to the channel vectors in each wideband RB. For supporting the ℓ -th wideband RB, the first 2D DFT beam is chosen as

$$\mathbf{c}_{1|\ell} = \mathbf{c}_1^v \otimes \mathbf{c}_1^h, \quad (27)$$

$$(\mathbf{c}_1^v, \mathbf{c}_1^h) = \arg \max_{(\tilde{\mathbf{c}}^v, \tilde{\mathbf{c}}^h) \in \mathcal{A}_{B_{W1}}^v \times \mathcal{A}_{B_{W1}}^h} \left\| \mathbf{H}_\ell^H (\tilde{\mathbf{c}}^v \otimes \tilde{\mathbf{c}}^h) \right\|_2^2$$

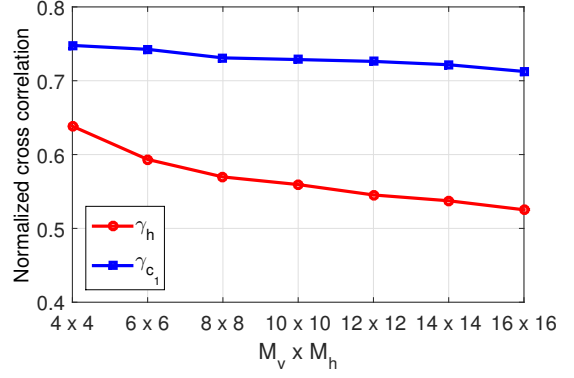


Fig. 3. Normalized beamforming gains between subcarrier channel vectors. ($B = 5$, $d_v = 0.8\lambda$, $d_h = 0.5\lambda$, $w \in \{1, \dots, 150\}$)

with B_{W1} -bit DFT codebooks. Next, the second 2D DFT beam is chosen using B_{W2} -bit DFT codebooks as

$$\mathbf{c}_{2|\ell} = \mathbf{c}_2^v \otimes \mathbf{c}_2^h, \quad (28)$$

$$(\mathbf{c}_2^v, \mathbf{c}_2^h) = \arg \max_{\tilde{\mathbf{c}}^v, \tilde{\mathbf{c}}^h} \max_{\tilde{\mathbf{z}} \in \mathcal{Z}_{B_c}} \left\| \frac{\mathbf{H}_\ell^H [\mathbf{c}_{1|\ell}, \tilde{\mathbf{c}}^v \otimes \tilde{\mathbf{c}}^h] \tilde{\mathbf{z}}}{\|[\mathbf{c}_{1|\ell}, \tilde{\mathbf{c}}^v \otimes \tilde{\mathbf{c}}^h] \tilde{\mathbf{z}}\|_2} \right\|_2^2$$

over $(\tilde{\mathbf{c}}^v, \tilde{\mathbf{c}}^h) \in \mathcal{A}_{B_{W2}}^v \times \mathcal{A}_{B_{W2}}^h$.

Level 2 (Narrowband resource block): Within the ℓ -th wideband RB, the set of 2D DFT beams $\mathbf{c}_{1|\ell}$ and $\mathbf{c}_{2|\ell}$ will be a baseline that guide the quantization of channel vectors in each narrowband RB. To construct each set of two codeword candidates, $2B_{N1}$ -bits are allocated for each narrowband RB.

Round 1: The first codeword is computed to support the channel scenario having a single dominant beam. The first codeword quantizes channel vectors $\mathbf{H}_{\ell,r}$ in the $r = \lceil R(\frac{wL}{W} - \ell - 1) \rceil$ -th narrowband RB of the $\ell = \lceil \frac{wL}{W} \rceil$ -th wideband RB by refining the beam direction of $\mathbf{c}_{1|\ell}$ according to

$$\mathbf{f}_{1|\ell,r} = \check{\mathbf{d}}_M(\theta_1^v, \theta_1^h) \odot \mathbf{c}_{1|\ell},$$

$$(\theta_1^v, \theta_1^h) = \arg \max_{\tilde{\theta}^v, \tilde{\theta}^h \in \mathcal{T}_{B_{W1}}^{B_{N1}}} \left\| \mathbf{H}_{\ell,r}^H (\check{\mathbf{d}}_M(\tilde{\theta}^v, \tilde{\theta}^h) \odot \mathbf{c}_{1|\ell}) \right\|_2^2$$

with B_{N1} -bit codebooks in (25).

Round 2: The second codeword is computed to support the channel scenario having two dominant beams. The proposed quantizer only refines the direction of $\mathbf{c}_{1|\ell}$ as well as combines with the second 2D DFT beam $\mathbf{c}_{2|\ell}$. The second codeword is

$$\mathbf{f}_{2|\ell,r} = \frac{[\check{\mathbf{d}}_M(\theta_2^v, \theta_2^h) \odot \mathbf{c}_{1|\ell}, \mathbf{c}_{2|\ell}] \mathbf{z}}{\|[\check{\mathbf{d}}_M(\theta_2^v, \theta_2^h) \odot \mathbf{c}_{1|\ell}, \mathbf{c}_{2|\ell}] \mathbf{z}\|_2},$$

$$(\theta_2^v, \theta_2^h, \mathbf{z}) = \arg \max_{\tilde{\theta}^v, \tilde{\theta}^h, \tilde{\mathbf{z}}} \left\| \frac{\mathbf{H}_{\ell,r}^H [\check{\mathbf{d}}_M(\tilde{\theta}^v, \tilde{\theta}^h) \odot \mathbf{c}_{1|\ell}, \mathbf{c}_{2|\ell}] \tilde{\mathbf{z}}}{\|[\check{\mathbf{d}}_M(\tilde{\theta}^v, \tilde{\theta}^h) \odot \mathbf{c}_{1|\ell}, \mathbf{c}_{2|\ell}] \tilde{\mathbf{z}}\|_2} \right\|_2^2$$

over $\tilde{\theta}^v, \tilde{\theta}^h \in \mathcal{T}_{B_{W1}}^{B_{N2}}$ in (25) and $\tilde{\mathbf{z}} \in \mathcal{Z}_{B_c}$. Out of $2B_{N1}$ -bits allocated for each narrowband RB, $2B_{N2}$ bits are assigned for refining the first 2D DFT beam and B_c bits are assigned for combining the two 2D DFT beams.

Round 3: Among the two codeword candidates, the final codeword is selected with an additional bit according to

$$\mathbf{f}_{\ell,r} = \arg \max_{\tilde{\mathbf{f}} \in \{\mathbf{f}_{1|\ell,r}, \mathbf{f}_{2|\ell,r}\}} \left\| \mathbf{H}_{\ell,r}^H \tilde{\mathbf{f}} \right\|_2^2. \quad (29)$$

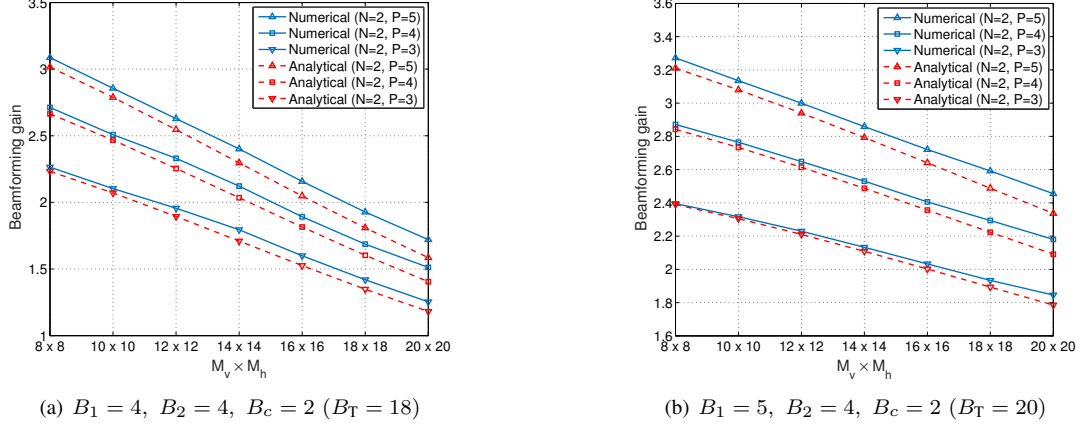


Fig. 4. Beamforming gain comparison between the numerical results G in (20) and the analytical results $G(M, P, N, \mathbf{r}_N)$ in (21).

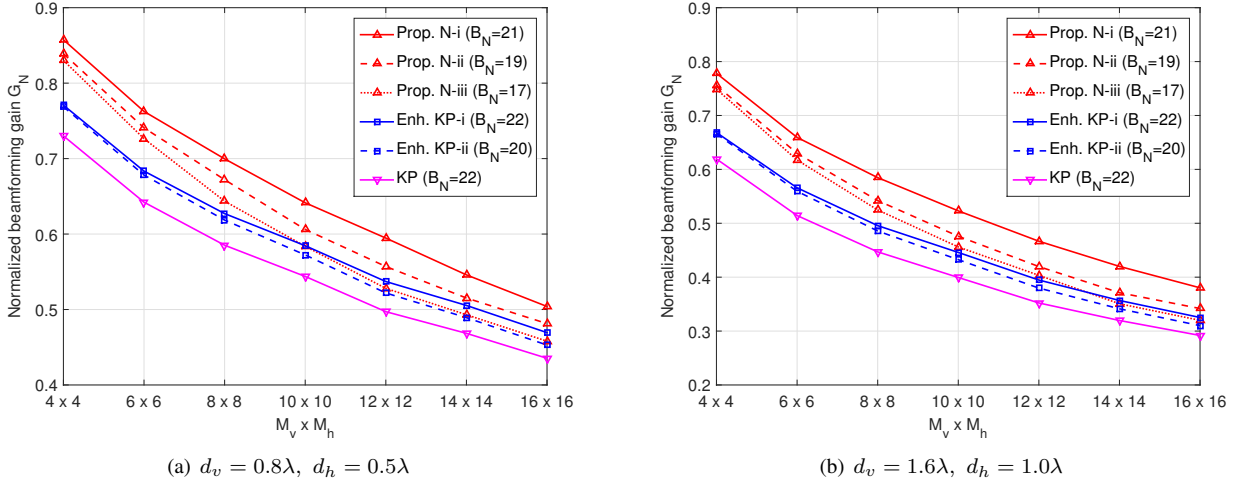


Fig. 5. Normalized beamforming gain of narrowband quantizers.

VI. SIMULATION RESULTS

We verify the performance of our CSI quantizers. Before evaluating the proposed quantizers, we pause to validate the accuracy of the approximated beamforming gain in (21). The beamforming gain between the simplified channel \mathbf{h} and the quantized channel $\mathbf{Cz}/\|\mathbf{Cz}\|_2$ is computed as in (20). For numerical simulations, 10,000 channels in (6) are generated by assuming a fixed number of the ray-like beams $P \in \{3, 4, 5\}$. In Fig. 4, it is shown that the approximated formula in (21) gives a tight lower bound on the numerical results in (20).

We now evaluate the narrowband quantizers using simulations. Numerical results are obtained through Monte Carlo simulations with 10,000 channel realizations. For generating 3D-SCM channels, we use the parameters in Table I. We evaluate the normalized beamforming gain of narrowband quantizer

$$G_N \doteq \mathbb{E}_{\mathbf{h}} [\|\mathbf{f}^H \mathbf{h} / \|\mathbf{h}\|_2\|^2],$$

where \mathbf{f} is the final codeword that is chosen in (26). We compare the beamforming gains of the proposed quantizer with that of the KP codebooks in [6], [7] and the enhanced KP codebook

TABLE I
3D-SCM SIMULATION PARAMETERS.

Tx antennas	4×4 to 20×20 Co-polarized UPA
Rx antennas	1 Co-polarized UPA
Scenario	UMi NLOS
Carrier frequency f_c	2 GHz
Subcarrier spacing Δ	15 KHz
Vertical antenna spacing d_v	$0.8\lambda_c, 1.6\lambda_c$
Horizontal antenna spacing d_h	$0.5\lambda_c, 1.0\lambda_c$

in [9]. Note that the feedback-bit allocation⁶ of each quantizer is listed in Table II and the computational complexity⁷ V_N and feedback overhead⁸ B_N are summarized in Table III.

In Figs. 5(a) and 5(b), the normalized beamforming gains of the three quantizers are plotted with different antenna spacing scenarios. The proposed quantizer searches both vertical and

⁶The feedback-bit allocation scenarios for the proposed narrowband quantizers are predefined in (23).

⁷We count the number of vector computations to evaluate the complexity.

⁸The feedback overhead (per each frequency tone CSI) is assessed by the combination of the overheads for both the first and second rounds in Section IV-D.

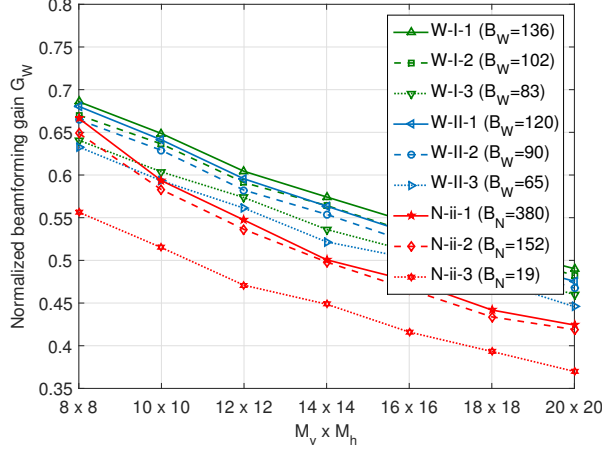
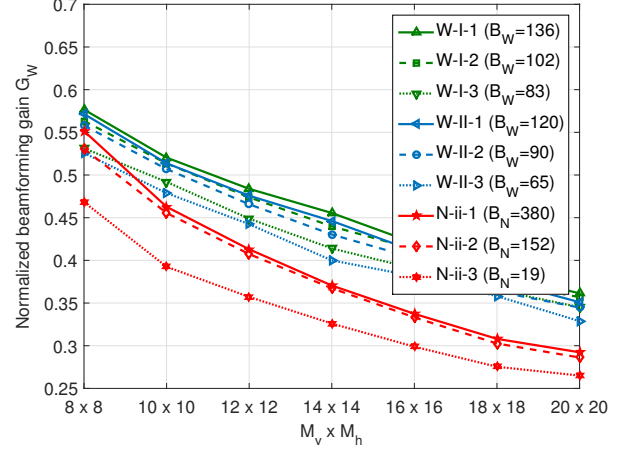
(a) $d_v = 0.8\lambda$, $d_h = 0.5\lambda$ (b) $d_v = 1.6\lambda$, $d_h = 1.0\lambda$

Fig. 6. Normalized beamforming gain comparison between the narrowband and wideband quantizers.

TABLE II
FEEDBACK CONFIGURATIONS OF NARROWBAND QUANTIZER

	1 st round	2 nd round	B_N	V_N
Prop. N-i	$B_1 = 5$	$\tilde{B}_1 = 5, B_2 = 4, B_c = 2$	21	3,072
Prop. N-ii	$B_1 = 5$	$\tilde{B}_1 = 4, B_2 = 3, B_c = 2$	19	1,536
Prop. N-iii	$B_1 = 4$	$\tilde{B}_1 = 4, B_2 = 3, B_c = 2$	17	768
Enh. KP-i	$B_1 + B_2$	$B_1 = 5, B_2 = 5$	22	2,176
Enh. KP-ii	$B_1 + B_2$	$B_1 = 5, B_2 = 4$	20	1,120
KP codebook	$B_1 = 11$		22	4,096

TABLE III
FEEDBACK OVERHEADS AND COMPLEXITY COMPARISONS

	Feedback overhead B_N	Vector computations V_N
Prop. quantizer	$2(B_1 + B_2) + B_c + 1$	$2^{2B_1} + 2^{2B_2 + B_c + 1}$
Enhanced KP	$2(B_1 + B_2 + 1)$	$2(2^{B_1 + B_2} + 2^{B_1} + 2^{B_2})$
KP codebook	$2B_1$	$2^{B_1 + 1}$

horizontal domains jointly, while other KP codebooks search beams lying in each domain independently and integrate the results later. The 2D DFT beams, which are quantized in the proposed quantizer, are aligned by cophasing and scaling each beam. On the contrary, the quantized beams in the enhanced KP codebook [9] are simply added up together without considering phase alignment. For these reasons, the proposed quantizer generates higher beamforming gains than those of other KP codebooks.

We next evaluate the normalized beamforming gain of the wideband quantizer according to

$$G_W \doteq E_{\mathbf{h}[w]} \left[\left| \mathbf{f}_{\ell,r}^H \mathbf{h}[w] / \|\mathbf{h}[w]\|_2 \right|^2 \right],$$

where $\mathbf{f}_{\ell,r}$ is the chosen codeword in (29). In Figs. 6(a) and 6(b), the normalized beamforming gains of wideband quantizer are compared with those of the narrowband quantizers. In the legend, the first alphabet denotes the type of quantizer, the second alphabet denotes the feedback-bit allocation scenario in Table IV, and the final digit represents the wideband

TABLE IV
FEEDBACK OVERHEADS FOR EACH WIDEBAND AND NARROWBAND RB

	Level 1: Wideband RB	Level 2: Narrowband RB
W-I	$B_{W1} = 5, B_{W2} = 5$	$B_{N1} = 3, B_{N2} = 2, B_c = 2$
W-II	$B_{W1} = 5, B_{W2} = 5$	$B_{N1} = 2, B_{N2} = 1, B_c = 2$

TABLE V
WIDEBAND CONFIGURATIONS FOR NARROWBAND AND WIDEBAND QUANTIZERS

	Narrowband quantizer	Wideband quantizer
N-1	1 codeword / 30 tones	W-1 $L = 4, R = 2$
N-2	1 codeword / 75 tones	W-2 $L = 3, R = 2$
N-3	1 codeword / 600 tones	W-3 $L = 1, R = 9$

configuration⁹ in Table V. The total feedback overhead of the proposed wideband quantizer is defined as

$$B_W = 2(B_{W1} + B_{W2})L + (2B_{N1} + 1)RL.$$

Numerical results verify that wideband quantizers outperform narrowband quantizers because it exploits correlation between frequency tone CSIs. The wideband quantizers also reduce feedback overhead because they can maintain quantization performance with less overhead compared to narrowband quantizers.

VII. CONCLUSION

In this paper, advanced CSI quantizers based on the KP codebook structure are proposed for FD-MIMO systems using UPAs. In the proposed quantizer designs, we focused on detecting and quantizing a limited number of dominant 2D beams in 3D channel vectors by exploiting DFT codebooks. The codebook for combiners was designed to cophase and scale the quantized 2D DFT beams. Furthermore, we analytically derived a design guideline for practical quantizers, which is based on FD-MIMO systems with predefined feedback-bit allocation scenarios.

⁹In the LTE setup of scheme W-3, the first 8 narrowband RBs have 72 tone CSIs and the ninth narrowband RB has 24 tone CSIs.

We then developed CSI quantizers by taking the predefined feedback scenarios into account. First, a narrowband quantizer was proposed to quantize and/or combine one or two dominant 2D DFT beams. To detect and quantize beams properly, we also developed a multi-round beam search approach that scans both vertical and horizontal domains jointly under the moderate computational complexity. To reduce total feedback overhead, we also proposed a wideband quantizer that utilizes the correlated information between multiple frequency tones. Numerical simulations verified that the proposed narrowband quantizer gives better quantization performance than previous CSI quantization techniques, and the proposed wideband quantizer further improves the quantization performance with less feedback overhead compared to the narrowband quantizer in wideband settings.

APPENDIX A CORRELATION BETWEEN ARRAY RESPONSE VECTOR AND DFT CODEWORD

We discuss the correlation between the array response vector in the domain a and the selected DFT codeword to quantify the quantization performance of DFT codebooks by evaluating

$$\begin{aligned}\Gamma_{na}^2 &\doteq \mathbb{E}[\|\mathbf{d}_{M_a}^H(\psi_n^a)\mathbf{c}_n^a\|^2] \\ &= \mathbb{E}\left[\max_{q \in \{1, \dots, Q_n\}} |\mathbf{d}_{M_a}^H(\psi_n^a)\mathbf{a}_{M_a}(q/Q_n)|^2\right] \\ &= \frac{1}{M_a^2} \mathbb{E}\left[\max_{q \in \{1, \dots, Q_n\}} \left|\sum_{m=0}^{M_a-1} e^{-j\pi m(\psi_n^a - 2q/Q_n + 1)}\right|^2\right] \\ &\stackrel{(a)}{=} \frac{1}{M_a^2} \mathbb{E}\left[\left|\sum_{m=0}^{M_a-1} e^{-j\pi m(\psi_n^a - 2q_n/Q_n + 1)}\right|^2\right],\end{aligned}$$

where (a) is rewritten with the index of selected codeword

$$q_n = \arg \min_{q \in \{1, \dots, Q_n\}} |\psi_n^a - 2q/Q_n + 1|.$$

The expectation over $\psi_n^a \sim \mathcal{U}(-1, 1)$ is rewritten by defining the new random variable as $\psi \doteq \psi_n^a - 2q_n/Q_n + 1$, which follows $\mathcal{U}(-1/Q_n, 1/Q_n)$ because $|\psi_n^a - 2q_n/Q_n + 1| \leq 1/Q_n$. Then, the formula is computed over ψ , as

$$\begin{aligned}\frac{1}{M_a^2} \mathbb{E}\left[\left|\sum_{m=0}^{M_a-1} e^{-j\pi m\psi}\right|^2\right] &= \frac{1}{M_a^2} \mathbb{E}\left[\sum_{\ell=0}^{M_a-1} \sum_{m=0}^{M_a-1} e^{-j\pi(m-\ell)\psi}\right] \\ &= \frac{1}{M_a^2} \left(M_a + \sum_{\ell=0}^{M_a-1} \sum_{m>\ell}^{M_a-1} \int_{-\frac{1}{Q_n}}^{\frac{1}{Q_n}} \frac{2 \cos(\pi(m-\ell)\psi)}{2/Q_n} d\psi\right) \\ &= \frac{1}{M_a^2} \left(M_a + \sum_{\ell=0}^{M_a-1} \sum_{m>\ell}^{M_a-1} \frac{2 \sin(\pi(m-\ell)/Q_n)}{\pi(m-\ell)/Q_n}\right) \\ &= \frac{1}{M_a^2} \left(M_a + \sum_{q=1}^{M_a-1} \frac{2(M_a - q) \sin(\pi q/Q_n)}{\pi q/Q_n}\right).\end{aligned}$$

APPENDIX B

LOWER BOUND OF NORMALIZED BEAMFORMING GAIN

Remark 2: To simplify analysis, we consider the first order Taylor expansion of the bivariate variables, which is derived as in [38],

$$\frac{A}{B} \simeq \frac{\mathbb{E}[A]}{\mathbb{E}[B]} + \frac{\partial(\frac{\mathbb{E}[A]}{\mathbb{E}[B]})}{\partial A}(A - \mathbb{E}[A]) + \frac{\partial(\frac{\mathbb{E}[A]}{\mathbb{E}[B]})}{\partial B}(B - \mathbb{E}[B]).$$

Expectation of the bivariate variables is then approximated as

$$\mathbb{E}\left[\frac{A}{B}\right] \simeq \mathbb{E}\left[\frac{\mathbb{E}[A]}{\mathbb{E}[B]}\right] = \frac{\mathbb{E}[A]}{\mathbb{E}[B]}.$$

The beamforming gain G^{bq} in Lemma 1 is lower bounded as

$$\begin{aligned}G^{\text{bq}} &= \mathbb{E}\left[\max_{\tilde{\mathbf{z}} \in \mathbb{C}^N} \frac{|\mathbf{h}^H \mathbf{C} \tilde{\mathbf{z}}|^2}{\|\mathbf{C} \tilde{\mathbf{z}}\|_2^2}\right] \\ &\stackrel{(a)}{\geq} \mathbb{E}\left[\frac{\max_{\tilde{\mathbf{z}} \in \mathbb{C}^N} |\mathbf{h}^H \mathbf{C} \tilde{\mathbf{z}}|^2}{\|\mathbf{C}\|_2^2}\right] \\ &\stackrel{(b)}{=} \mathbb{E}\left[\frac{\|\mathbf{h}^H \mathbf{C}\|_2^2}{\|\mathbf{C}\|_2^2}\right] \\ &\stackrel{(c)}{\simeq} \frac{\mathbb{E}[\|\mathbf{h}^H \mathbf{C}\|_2^2]}{\mathbb{E}[\|\mathbf{C}\|_2^2]},\end{aligned}\tag{30}$$

where the inequality in (a) is based on $\|\mathbf{C} \tilde{\mathbf{z}}\|_2^2 \leq \|\mathbf{C}\|_2^2 \|\tilde{\mathbf{z}}\|_2^2$ and $\|\tilde{\mathbf{z}}\|_2^2 = 1$, (b) holds when $\tilde{\mathbf{z}} \doteq \mathbf{C}^H \mathbf{h} / \|\mathbf{C}^H \mathbf{h}\|_2$, and (c) is derived based on Remark 2.

To complete the lower bound in (30), we first compute the expectation of two-norm squared of the effective channel vector

$$\begin{aligned}\mathbb{E}[\|\mathbf{h}^H \mathbf{C}\|_2^2] &= \mathbb{E}\left[\|\mathbf{h}^H [\mathbf{c}_1^v \otimes \mathbf{c}_1^h, \dots, \mathbf{c}_N^v \otimes \mathbf{c}_N^h]\|_2^2\right] \\ &= \sum_{n=1}^N \mathbb{E}\left[\|\mathbf{h}^H (\mathbf{c}_n^v \otimes \mathbf{c}_n^h)\|^2\right] \\ &\stackrel{(a)}{=} \frac{1}{M} \left(PN + \sum_{n=1}^N \sum_{q=n}^P \frac{M \Gamma_{nv}^2 \Gamma_{nh}^2 - 1}{q}\right),\end{aligned}\tag{31}$$

where (a) is derived by using the correlation between the channel vector and the n -th selected DFT codeword $\mathbb{E}[\|\mathbf{h}^H (\mathbf{c}_n^v \otimes \mathbf{c}_n^h)\|^2]$ that will be discussed in Appendix E.

We next consider the set of N DFT vectors \mathbf{C} in (12). The expectation of two-norm squared of \mathbf{C} is approximated as

$$\begin{aligned}\mathbb{E}[\|\mathbf{C}\|_2^2] &= \mathbb{E}\left[\max_{\tilde{\mathbf{x}} \in \mathbb{C}^N} \tilde{\mathbf{x}}^H (\mathbf{C}^H \mathbf{C}) \tilde{\mathbf{x}}\right] \\ &\simeq \max_{\tilde{\mathbf{x}} \in \mathbb{C}^N} \tilde{\mathbf{x}}^H \mathbb{E}[\mathbf{C}^H \mathbf{C}] \tilde{\mathbf{x}}\end{aligned}\tag{32}$$

subject to $\|\tilde{\mathbf{x}}\|_2^2 = 1$. Note that $\mathbb{E}[\mathbf{C}^H \mathbf{C}]$ is computed as

$$\begin{aligned}\mathbb{E}\left[\begin{array}{cccc} (\mathbf{c}_1^v)^H \mathbf{c}_1^v \otimes (\mathbf{c}_1^h)^H \mathbf{c}_1^h & \dots & (\mathbf{c}_1^v)^H \mathbf{c}_N^v \otimes (\mathbf{c}_1^h)^H \mathbf{c}_N^h \\ \vdots & \ddots & \vdots \\ (\mathbf{c}_N^v)^H \mathbf{c}_1^v \otimes (\mathbf{c}_N^h)^H \mathbf{c}_1^h & \dots & (\mathbf{c}_N^v)^H \mathbf{c}_N^v \otimes (\mathbf{c}_N^h)^H \mathbf{c}_N^h \end{array}\right] \\ = \begin{bmatrix} 1 & \dots & \frac{1}{M_v M_h} \\ \vdots & \ddots & \vdots \\ \frac{1}{M_v M_h} & \dots & 1 \end{bmatrix}\end{aligned}\tag{33}$$

$$\begin{aligned}
\mathbb{E}[(\mathbf{c}_c^v \otimes \mathbf{c}_c^h)^H \mathbf{h} \mathbf{h}^H (\mathbf{c}_d^v \otimes \mathbf{c}_d^h)] &= \left(\sum_{p=1}^P \alpha_p^* (\mathbf{d}_{M_v}^H(\psi_p^v) \mathbf{c}_c^v) (\mathbf{d}_{M_v}^H(\psi_p^h) \mathbf{c}_c^h) \right)^* \left(\sum_{q=1}^P \alpha_q^* (\mathbf{d}_{M_v}^H(\psi_q^v) \mathbf{c}_d^v) (\mathbf{d}_{M_v}^H(\psi_q^h) \mathbf{c}_d^h) \right) \\
&= \sum_{p=1}^P \mathbb{E}[|\alpha_p|^2] \mathbb{E}[(\mathbf{c}_c^v)^H \mathbf{d}_{M_v}(\psi_p^v) \mathbf{d}_{M_v}^H(\psi_p^v) \mathbf{c}_c^v] \mathbb{E}[(\mathbf{c}_c^h)^H \mathbf{d}_{M_v}(\psi_p^h) \mathbf{d}_{M_v}^H(\psi_p^h) \mathbf{c}_c^h]. \quad (36)
\end{aligned}$$

where $\mathbf{c}_n^a = \mathbf{a}_{M_a}(q_n/Q_n)$ with $Q_n = 2^{B_n}$ is chosen as in (15). Because we assume that beam directions are uniformly distributed $\psi_n^a \sim \mathcal{U}(-1, 1)$, \mathbf{c}_n^a can be chosen as one of $Q_n = 2^{B_n}$ codewords in the DFT codebook $\mathcal{A}_{B_n}^a$ with equal probabilities. For this reason, we can obtain $\mathbb{E}[(\mathbf{c}_c^a)^H \mathbf{c}_d^a]$ in (33) by computing its arithmetic mean of the beamforming gain between two different codewords ($c \neq d$) as

$$\begin{aligned}
\mathbb{E}[(\mathbf{c}_c^a)^H \mathbf{c}_d^a] &= \frac{1}{Q_c Q_d} \sum_{q_c=1}^{Q_c} \sum_{q_d=1}^{Q_d} \mathbf{a}_{M_a}^H(q_c/Q_c) \mathbf{a}_{M_a}(q_d/Q_d) \\
&= \frac{1}{M_a Q_c Q_d} \left[\sum_{q_c=1}^{Q_c} \sum_{q_d=1}^{Q_d} 1 + \sum_{m=1}^{M_a-1} \sum_{q_c=1}^{Q_c} \sum_{q_d=1}^{Q_d} e^{\frac{j2\pi m q_d}{Q_d}} e^{-\frac{j2\pi m q_c}{Q_c}} \right] \\
&= \frac{1}{M_a Q^2} \left[Q^2 + \sum_{m=1}^{M_a-1} \left(\frac{1 - e^{j2\pi m}}{1 - e^{\frac{j2\pi m}{Q_d}}} \right) \left(\frac{1 - e^{-j2\pi m}}{1 - e^{-\frac{j2\pi m}{Q_c}}} \right) \right] \\
&= \frac{1}{M_a}. \quad (34)
\end{aligned}$$

Based on $\mathbb{E}[\mathbf{C}^H \mathbf{C}]$, the expectation of two-norm squared of \mathbf{C} in (32) is approximated as

$$\begin{aligned}
\mathbb{E}[\|\mathbf{C}\|_2^2] &\simeq \text{eig}_{\max}\{\mathbb{E}[\mathbf{C}^H \mathbf{C}]\} \\
&= \frac{\text{eig}_{\max}\{\mathbf{1}_{N,N}\}}{M} + \frac{M-1}{M} \\
&\stackrel{(a)}{=} \frac{M+N-1}{M}, \quad (35)
\end{aligned}$$

where (a) is derived because $\text{eig}_{\max}\{\mathbf{1}_{N,N}\} = N$, which holds when $\hat{\mathbf{x}} = \frac{1}{\sqrt{N}}[1, \dots, 1]^T \in \mathbb{C}^N$.

Finally, the lower bound of G^{bq} in (30) is approximated by plugging the derived formulas in (31) and (35) into (30) as

$$G^{\text{bq}} \simeq \frac{P}{M+N-1} \left(N + \sum_{n=1}^N \sum_{q=n}^P \frac{M \Gamma_{nv}^2 \Gamma_{nh}^2 - 1}{qP} \right).$$

APPENDIX C

COVARIANCE MATRIX OF EFFECTIVE CHANNEL VECTOR

Each entry of \mathbf{R} in (18) is rewritten in (36). Note that $\mathbb{E}[(\mathbf{c}_c^a)^H \mathbf{d}_{M_a}(\psi_p^a) \mathbf{d}_{M_a}^H(\psi_p^a) \mathbf{c}_d^a]$ in (36) is computed depending on the different cases as follows:

Case 1: $p = c = d$.

$$\mathbb{E}[(\mathbf{c}_c^a)^H \mathbf{d}_{M_a}(\psi_p^a) \mathbf{d}_{M_a}^H(\psi_p^a) \mathbf{c}_d^a] = \Gamma_{ac}^2,$$

where Γ_{ac}^2 is derived in Appendix A.

Case 2: $p \neq c, c = d$.

$$\begin{aligned}
\mathbb{E}[(\mathbf{c}_c^a)^H \mathbf{d}_{M_a}(\psi_p^a) \mathbf{d}_{M_a}^H(\psi_p^a) \mathbf{c}_d^a] &= \mathbb{E}[|\mathbf{d}_{M_a}^H(\psi_p^a) \mathbf{a}_{M_a}(q_c/Q_c)|^2] \\
&\stackrel{(a)}{=} \frac{1}{M_a},
\end{aligned}$$

where q_c is chosen as in (15). Note that (a) is derived by computing the arithmetic mean.

Case 3: $p = c, c \neq d$.

$$\begin{aligned}
\mathbb{E}[(\mathbf{c}_c^a)^H \mathbf{d}_{M_a}(\psi_p^a) \mathbf{d}_{M_a}^H(\psi_p^a) \mathbf{c}_d^a] &= \Gamma_{ac} \mathbb{E}[\mathbf{d}_{M_a}^H(\psi_c^a) \mathbf{c}_d^a] \\
&\stackrel{(a)}{=} \frac{\Gamma_{ac}}{M_a},
\end{aligned}$$

where (a) is derived because

$$\begin{aligned}
\mathbb{E}[\mathbf{d}_{M_a}^H(\psi_c^a) \mathbf{c}_d^a] &= \mathbb{E}[\mathbf{d}_{M_a}^H(\psi_c^a) \mathbf{a}_{M_a}(q_d/Q_d)] \\
&= \frac{1}{M_a} \sum_{m=0}^{M_a-1} \mathbb{E}\left[e^{-j\pi m(\psi_c^a - \frac{2q_d}{Q_d} + 1)}\right] \\
&\stackrel{(b)}{=} \frac{1}{M_a} \sum_{m=0}^{M_a-1} \int_{-1}^1 \frac{e^{-j\pi m\phi}}{2} d\phi \\
&= \frac{1}{M_a}.
\end{aligned}$$

Note that (b) is derived because $\phi, \psi_c^a \sim \mathcal{U}(-1, 1)$ with the definition of $\phi \doteq \psi_c^a - \frac{2q_d}{Q_d} + 1$ for any $q_d \in \{1, \dots, Q_d\}$ in (15).

Case 4: $p \neq c, p \neq d, c \neq d$.

$$\begin{aligned}
\mathbb{E}[(\mathbf{c}_c^a)^H \mathbf{d}_{M_a}(\psi_p^a) \mathbf{d}_{M_a}^H(\psi_p^a) \mathbf{c}_d^a] &= \frac{1}{M_a^2} \mathbb{E}\left[\sum_{\ell=0}^{M_a-1} e^{j\pi\ell(\psi_p^a - \frac{2q_c}{Q_c} + 1)} \sum_{m=0}^{M_a-1} e^{-j\pi m(\psi_p^a - \frac{2q_d}{Q_d} + 1)}\right] \\
&= \frac{1}{M_a^2} \sum_{\ell=0}^{M_a-1} \sum_{m=0}^{M_a-1} e^{j\pi(\ell-m)} \\
&\quad \mathbb{E}\left[e^{j2\pi(\frac{mq_d}{Q_d} - \frac{\ell q_c}{Q_c})}\right] \int_{-1}^1 \frac{e^{j\pi(\ell-m)\psi_p^a}}{2} d\psi_p^a \\
&= \frac{1}{M_a^2} \sum_{m=0}^{M_a-1} \mathbb{E}\left[e^{j2\pi m(\frac{q_d}{Q_d} - \frac{q_c}{Q_c})}\right] \\
&\stackrel{(a)}{=} \frac{1}{M_a^2},
\end{aligned}$$

where (a) is derived by computing the arithmetic mean.

APPENDIX D

QUANTIZATION PERFORMANCE OF \mathcal{Z}_{B_c}

The normalized beamforming gain between the effective channel vector and the selected combiner is lower bounded as

$$\begin{aligned}
G^{\text{bc}} &= \mathbb{E}\left[\frac{|\mathbf{e}_{\hat{u}}^H \mathbf{R} \mathbf{w}|^2}{(\mathbf{w}^H \mathbf{R} \mathbf{w})(\mathbf{e}_{\hat{u}}^H \mathbf{R} \mathbf{e}_{\hat{u}})}\right] \\
&\stackrel{(a)}{=} \mathbb{E}\left[\frac{|\mathbf{e}_{\hat{u}}^H \mathbf{R}(\mathbf{e}_{\hat{u}} \cos \theta_{\hat{u}} + \mathbf{k}_{\hat{u}} \sin \theta_{\hat{u}})|^2}{(\mathbf{w}^H \mathbf{R} \mathbf{w})(\mathbf{e}_{\hat{u}}^H \mathbf{R} \mathbf{e}_{\hat{u}})}\right]
\end{aligned}$$

$$\begin{aligned}
&= \mathbb{E} \left[\left| \frac{\mathbf{e}_{\hat{u}}^H \mathbf{R} \mathbf{e}_{\hat{u}}}{\mathbf{w}^H \mathbf{R} \mathbf{w}} \right| 1 + \left| \frac{\mathbf{e}_{\hat{u}}^H \mathbf{R} \mathbf{k}_{\hat{u}}}{\mathbf{e}_{\hat{u}}^H \mathbf{R} \mathbf{e}_{\hat{u}}} \right| \tan \theta_{\hat{u}} e^{j \angle \mathbf{e}_{\hat{u}}^H \mathbf{R} \mathbf{k}_{\hat{u}}} \right]^2 \cos^2 \theta_{\hat{u}} \\
&\stackrel{(b)}{\approx} \mathbb{E} \left[\frac{\mathbf{e}_{\hat{u}}^H \mathbf{R} \mathbf{e}_{\hat{u}} \cos^2 \theta_{\hat{u}}}{\mathbf{w}^H \mathbf{R} \mathbf{w}} \right] \\
&\stackrel{(c)}{\approx} \frac{\mathbb{E}[\mathbf{e}_{\hat{u}}^H \mathbf{R} \mathbf{e}_{\hat{u}} \cos^2 \theta_{\hat{u}}]}{\mathbb{E}[\mathbf{w}^H \mathbf{R} \mathbf{w}]} \quad (37)
\end{aligned}$$

In (37), (a) is based on $\mathbf{w} \doteq \mathbf{e}_{\hat{u}} \cos \theta_{\hat{u}} + \mathbf{k}_{\hat{u}} \sin \theta_{\hat{u}}$ with $\mathbf{e}_{\hat{u}} \perp \mathbf{k}_{\hat{u}}$, (b) is approximated because $|\mathbf{e}_{\hat{u}}^H \mathbf{R} \mathbf{k}_{\hat{u}}| \ll |\mathbf{e}_{\hat{u}}^H \mathbf{R} \mathbf{e}_{\hat{u}}|$ and $\tan \theta_{\hat{u}} \ll 1$, and (c) is approximated based on Remark 2 in Appendix B.

Although G^{bc} is simplified in (37), it is still difficult to solve in most cases. In the special case of $N = 2$, the equal gain vectors can be defined as

$$\mathbf{w} \doteq \frac{e^{j\nu}}{\sqrt{2}}[1, e^{j\nu}]^T, \quad \mathbf{e}_u \doteq \frac{1}{\sqrt{2}}[1, e^{j\frac{2\pi u}{U}}]^T$$

using $\nu, u \sim \mathcal{U}(-\pi, \pi)$, and the beamforming gain in (37) is then derived such as

$$\begin{aligned}
&\frac{\mathbb{E}[\mathbf{e}_{\hat{u}}^H \mathbf{R} \mathbf{e}_{\hat{u}} \cos^2 \theta_{\hat{u}}]}{\mathbb{E}[\mathbf{w}^H \mathbf{R} \mathbf{w}]} \stackrel{(a)}{=} \frac{\mathbb{E}[\mathbf{e}_{\hat{u}}^H \mathbf{R} \mathbf{e}_{\hat{u}} (1 + \cos \hat{\nu})]}{2\mathbb{E}[\mathbf{w}^H \mathbf{R} \mathbf{w}]} \\
&\stackrel{(b)}{=} \frac{\sum_{\ell=1}^U \mathbb{E}[\mathbf{e}_{\hat{u}}^H \mathbf{R} \mathbf{e}_{\hat{u}} (1 + \cos \hat{\nu}) \mid \hat{u} = \ell]}{2U\mathbb{E}[\mathbf{w}^H \mathbf{R} \mathbf{w}]} \\
&= \frac{\sum_{\ell=1}^U \frac{U}{2\pi} \int_{-\frac{\pi}{U}}^{\frac{\pi}{U}} \mathbf{e}_{\ell}^H \mathbf{R} \mathbf{e}_{\ell} (1 + \cos \tau) d\tau}{2U\mathbb{E}[\mathbf{w}^H \mathbf{R} \mathbf{w}]} \\
&= \frac{\frac{1}{U} \sum_{\ell=1}^U \mathbf{e}_{\ell}^H \mathbf{R} \mathbf{e}_{\ell}}{2\mathbb{E}[\mathbf{w}^H \mathbf{R} \mathbf{w}]} \left(1 + \frac{U}{\pi} \sin \frac{\pi}{U} \right) \\
&\stackrel{(c)}{=} \frac{1}{2} \left(1 + \frac{U}{\pi} \sin \frac{\pi}{U} \right).
\end{aligned}$$

Note that (a) is derived based on the definition $\hat{\nu} \doteq \nu - \frac{2\pi \hat{u}}{U}$ that follows $\mathcal{U}(-\frac{\pi}{U}, \frac{\pi}{U})$ because $|\nu - \frac{2\pi \hat{u}}{U}| \leq \frac{\pi}{U}$, $\nu \sim \mathcal{U}(-\pi, \pi)$, and $\hat{u} = \arg \min_{u \in \{1, \dots, U\}} |\nu - \frac{2\pi u}{U}|$ based on Assumption 2. In addition,

(b) is derived by computing its arithmetic mean because \hat{u} is equally probable from 1 to U , and (c) is derived because

$$\begin{aligned}
\mathbb{E}[\mathbf{w}^H \mathbf{R} \mathbf{w}] &= (\mathbf{R}_{1,1} + \mathbf{R}_{2,2})/2 + |\mathbf{R}_{1,2}| \mathbb{E}[\cos(\nu + \angle \mathbf{R}_{1,2})] \\
&= (\mathbf{R}_{1,1} + \mathbf{R}_{2,2})/2,
\end{aligned}$$

and the arithmetic mean of $\mathbf{e}_{\ell}^H \mathbf{R} \mathbf{e}_{\ell}$ is derived as

$$\begin{aligned}
\sum_{\ell=1}^U \frac{\mathbf{e}_{\ell}^H \mathbf{R} \mathbf{e}_{\ell}}{U} &= \frac{\mathbf{R}_{1,1} + \mathbf{R}_{2,2}}{2} + \sum_{\ell=1}^U \frac{|\mathbf{R}_{1,2}| \cos(\frac{2\pi \ell}{U} + \angle \mathbf{R}_{1,2})}{U} \\
&= (\mathbf{R}_{1,1} + \mathbf{R}_{2,2})/2.
\end{aligned}$$

APPENDIX E

CORRELATION BETWEEN CHANNEL VECTOR AND DFT CODEWORD

We derive a correlation between the channel in (6) and the n -th selected 2D DFT beam

$$\begin{aligned}
&\mathbb{E} \left[|\mathbf{h}^H (\mathbf{c}_n^v \otimes \mathbf{c}_n^h)|^2 \right] \\
&= \mathbb{E} \left[\left| \sum_{p=1}^P \alpha_p^* (\mathbf{d}_{M_v}^H(\psi_p^v) \mathbf{c}_n^v) (\mathbf{d}_{M_h}^H(\psi_p^h) \mathbf{c}_n^h) \right|^2 \right]
\end{aligned}$$

$$\begin{aligned}
&\stackrel{(a)}{=} \sum_{p=1}^P \mathbb{E}[|\alpha_p|^2] \mathbb{E}[|\mathbf{d}_{M_v}^H(\psi_p^v) \mathbf{c}_n^v|^2] \mathbb{E}[|\mathbf{d}_{M_h}^H(\psi_p^h) \mathbf{c}_n^h|^2] \\
&\stackrel{(b)}{=} \mathbb{E}[|\alpha_n|^2] \Gamma_{nv}^2 \Gamma_{nh}^2 + \sum_{p \neq n}^P \frac{\mathbb{E}[|\alpha_p|^2]}{M_v M_h} \\
&= \mathbb{E}[|\alpha_n|^2] \Gamma_{nv}^2 \Gamma_{nh}^2 + \frac{P - \mathbb{E}[|\alpha_n|^2]}{M}, \quad (38)
\end{aligned}$$

where $\Gamma_{na}^2 \doteq \mathbb{E}[|\mathbf{d}_{M_a}^H(\psi_n^a) \mathbf{c}_n^a|^2]$ is derived in Appendix A. Note that (a) is derived because $\mathbb{E}[\alpha_p^* \alpha_q] = 0$ when $p \neq q$ and (b) is derived because

$$\begin{aligned}
&\mathbb{E}[|\mathbf{d}_{M_a}^H(\psi_p^a) \mathbf{c}_n^a|^2] = \mathbb{E}[|\mathbf{d}_{M_a}^H(\psi_p^a) \mathbf{a}_{M_a}(q_n/Q_n)|^2] \\
&= \frac{1}{M_a^2} \mathbb{E} \left[\sum_{\ell=0}^{M_a-1} e^{j\pi \ell (\psi_p^a - \frac{2q_n}{Q_n} + 1)} \sum_{m=0}^{M_a-1} e^{-j\pi m (\psi_p^a - \frac{2q_n}{Q_n} + 1)} \right] \\
&= \frac{1}{M_a^2} \sum_{\ell=0}^{M_a-1} \sum_{m=0}^{M_a-1} \mathbb{E}[e^{j\pi (m-\ell) (\frac{2q_n}{Q_n} - 1)}] \int_{-1}^1 \frac{e^{j\pi (\ell-m) \psi_p^a}}{2} d\psi_p^a \\
&= \frac{1}{M_a^2} \sum_{m=0}^{M_a-1} \sum_{m=\ell}^{M_a-1} \mathbb{E}[e^{j\pi (m-\ell) (\frac{2q_n}{Q_n} - 1)}] \frac{\sin(\pi(\ell-m))}{\pi(\ell-m)} \\
&= \frac{1}{M_a}.
\end{aligned}$$

To complete the formula in (38), we compute the power of the n -th largest channel gain $\mathbb{E}[|\alpha_n|^2]$. Without loss of generality, we assume that the magnitude of channel gains are in descending order, i.e., $|\alpha_1|^2 \geq \dots \geq |\alpha_P|^2$. The channel gain $A \doteq |\alpha_p|^2$ follows χ_2^2 that is characterized by the cumulative distribution function (cdf) of

$$F_A(a) = 1 - e^{-a}$$

because $\alpha_p \sim \mathcal{CN}(0, 1)$. We now consider the k -th order statistic (k -th smallest order statistic) of P i.i.d exponentially distributed random variables $A_k \doteq |\alpha_{P-k+1}|^2$. Then, we refer to [39] for defining the pdf of A_k , yielding

$$\begin{aligned}
f_{A_k}(a) &= P \binom{P-1}{k-1} (1 - e^{-a})^{k-1} e^{-a(P-k+1)} \\
&\stackrel{(a)}{=} P \binom{P-1}{k-1} \sum_{q=0}^{k-1} \binom{k-1}{q} (-1)^q e^{-a(q+P-k+1)},
\end{aligned}$$

where (a) is derived based on the binomial expansion formula. Then, the expectation of k -th order statistic is defined as

$$\begin{aligned}
\mathbb{E}[A_k] &= \sum_{q=0}^{k-1} \frac{P! \binom{k-1}{q} (-1)^q}{(P-k)! (k-1)!} \int_0^\infty a e^{-a(q+P-k+1)} da \\
&= \sum_{q=P-k+1}^P \frac{P! (-1)^{q-(P-k+1)}}{(P-q)! q!} \left[\frac{(q-1) \dots (q-(P-k))}{q(P-k)!} \right] \\
&\stackrel{(a)}{=} \sum_{q=1}^P \frac{\binom{P}{q} (-1)^{q-(P-k+1)}}{q} \left[\frac{q-1}{1} \frac{q-2}{2} \dots \frac{q-(P-k)}{P-k} \right] \\
&\stackrel{(b)}{=} \left[\sum_{q=1}^P \binom{P}{q} (-1)^q \right] \sum_{\ell=1}^{P-k} \frac{1}{\ell} + \sum_{q=1}^P \frac{\binom{P}{q} (-1)^{q+1}}{q}
\end{aligned}$$

$$\begin{aligned}
& \stackrel{(c)}{=} \sum_{\ell=1}^{P-k} \frac{1}{\ell} \left[\sum_{q=0}^P \binom{P}{q} (-1)^q - \binom{P}{0} (-1)^0 \right] + \sum_{q=1}^P \frac{1}{q} \\
& \stackrel{(d)}{=} - \sum_{\ell=1}^{P-k} \frac{1}{\ell} + \sum_{q=1}^P \frac{1}{q} = \sum_{q=P-k+1}^P \frac{1}{q}.
\end{aligned}$$

Notice that (a) is derived because $\sum_{q=b}^P f(q)(q-b) = \sum_{q=b+1}^P f(q)(q-b) + f(b)(b-b)$ for any function $f(\cdot)$, (b) is derived because $\sum_{q=1}^P \frac{\binom{P}{q}(-1)^{q+1}}{q} = \sum_{q=1}^P \frac{\binom{P}{q}(-1)^{q-1}}{q}$, (c) is derived based on $\sum_{k=1}^n \frac{\binom{n}{k}(-1)^{k+1}}{\binom{n}{k}} = \sum_{k=1}^n \frac{1}{k}$, and (d) is derived based on $\sum_{k=0}^n (-1)^k \binom{n}{k} = 0$. We now compute the n -th largest channel gain as

$$E[|\alpha_n|^2] = E[A_{P-n+1}] = \sum_{q=n}^P \frac{1}{q}.$$

Finally, the correlation coefficient is rewritten by plugging $|\alpha_n|^2$ into (38).

$$E[|\mathbf{h}^H(\mathbf{c}_n^v \otimes \mathbf{c}_n^h)|^2] = \frac{1}{M} \left(P + \sum_{q=n}^P \frac{M\Gamma_{nv}^2 \Gamma_{nh}^2 - 1}{q} \right).$$

REFERENCES

- [1] J. Song, J. Choi, K. Lee, T. Kim, J. Y. Seol, and D. J. Love, "Advanced quantizer designs for FD-MIMO systems using uniform planar arrays," in *Proceedings of IEEE Global Telecommunications Conference*, Dec. 2016.
- [2] T. L. Marzetta, "Noncooperative cellular wireless with unlimited numbers of base station antennas," *IEEE Transactions on Wireless Communications*, vol. 9, no. 11, pp. 3590–3600, Nov. 2010.
- [3] R. C. Hansen, *Phased array antennas*, 2nd ed. Hoboken: Wiley-Interscience, 2009.
- [4] Y. H. Nam, B. L. Ng, K. Sayana, Y. Li, J. Zhang, Y. Kim, and J. Lee, "Full-dimension MIMO for next generation cellular technology," *IEEE Communications Magazine*, vol. 51, no. 6, pp. 172–179, Jun. 2013.
- [5] R1-150381, *Discussions on FD-MIMO codebook enhancements*, 3GPP TSG RAN WG1 #80 Std., Feb. 2015.
- [6] R1-150057, *Codebook enhancements for EBF/FD-MIMO*, 3GPP TSG RAN WG1 #80 Std., Feb. 2015.
- [7] R1-150560, *Codebook for 2D antenna arrays*, 3GPP TSG RAN WG1 #80 Std., Feb. 2015.
- [8] J. Li, X. Su, J. Zeng, Y. Zhao, S. Yu, L. Xiao, and X. Xu, "Codebook design for uniform rectangular arrays of massive antennas," in *Proceedings of IEEE Vehicular Technology Conference*, Jun. 2013.
- [9] J. Choi, K. Lee, D. J. Love, T. Kim, and R. W. Heath, "Advanced limited feedback designs for FD-MIMO using uniform planar arrays," in *Proceedings of IEEE Global Telecommunications Conference*, Dec. 2015.
- [10] J. Choi, T. Kim, D. J. Love, and J. Y. Seol, "Exploiting the preferred domain of FDD massive MIMO systems with uniform planar arrays," in *Proceedings of IEEE International Conference on Communications*, Jun. 2015.
- [11] H. Q. Ngo, E. G. Larsson, and T. L. Marzetta, "Massive MU-MIMO downlink TDD systems with linear precoding and downlink pilots," in *Proceedings of Allerton Conference on Communication, Control, and Computing*, Oct. 2013.
- [12] R. Rogalin, O. Y. Bursalioğlu, H. Papadopoulos, G. Caire, A. F. Molisch, A. Michaloliakos, V. Balan, and K. Psounis, "Scalable synchronization and reciprocity calibration for distributed multiuser MIMO," *IEEE Transactions on Wireless Communications*, vol. 13, no. 4, pp. 1815–1831, Mar. 2014.
- [13] B. Hassibi and B. M. Hochwald, "How much training is needed in multiple-antenna wireless links?" *IEEE Transactions on Information Theory*, vol. 49, no. 4, pp. 951–963, Apr. 2003.
- [14] C. K. Au-Yeung and D. J. Love, "On the performance of random vector quantization limited feedback beamforming in a MISO system," *IEEE Transactions on Wireless Communications*, vol. 6, no. 2, pp. 458–462, Feb. 2007.
- [15] C. K. Au-Yeung, D. J. Love, and S. Sanayei, "Trellis coded line packing: large dimensional beamforming vector quantization and feedback transmission," *IEEE Transactions on Wireless Communications*, vol. 10, no. 8, pp. 1844–1853, Apr. 2011.
- [16] J. Choi, A. Chance, D. J. Love, and U. Madhow, "Noncoherent trellis coded quantization: a practical limited feedback technique for massive MIMO systems," *IEEE Transactions on Communications*, vol. 61, no. 12, pp. 5016–5029, Dec. 2013.
- [17] J. Choi, D. J. Love, and T. Kim, "Trellis-extended codebooks and successive phase adjustment: a path from LTE-advanced to FDD massive MIMO systems," *IEEE Transactions on Wireless Communications*, vol. 14, no. 4, pp. 2007–2016, Apr. 2015.
- [18] J. Choi, D. J. Love, and P. Bidigare, "Downlink training techniques for FDD massive MIMO systems: open-loop and closed-loop training with memory," *IEEE Journal of Selected Topics in Signal Processing*, vol. 8, no. 5, pp. 802–814, Dec. 2014.
- [19] S. Noh, M. D. Zoltowski, Y. Sung, and D. J. Love, "Pilot beam pattern design for channel estimation in massive MIMO systems," *IEEE Journal of Selected Topics in Signal Processing*, vol. 8, no. 5, pp. 787–801, Oct. 2014.
- [20] Y. Han, J. Lee, and D. J. Love, "Compressed sensing-aided downlink channel training for FDD massive MIMO systems," to appear in *IEEE Transactions on Communications*, 2017.
- [21] K. K. Mukkavilli, A. Sabharwal, E. Erkip, and B. Aazhang, "On beamforming with finite rate feedback in multiple-antenna systems," *IEEE Transactions on Information Theory*, vol. 49, no. 10, pp. 2562–2579, Jan. 2003.
- [22] D. J. Love, R. W. Heath, and T. Strohmer, "Grassmannian beamforming for multiple-input multiple-output wireless systems," *IEEE Transactions on Information Theory*, vol. 49, no. 10, pp. 2735–2747, Oct. 2003.
- [23] D. J. Love, R. W. Heath, V. K. Lau, D. Gesbert, B. D. Rao, and M. Andrews, "An overview of limited feedback in wireless communication systems," *IEEE Journal on Selected Areas in Communications*, vol. 26, no. 8, pp. 1341–1365, Oct. 2008.
- [24] D. J. Love and R. W. Heath, "Grassmannian beamforming on correlated MIMO channels," in *Proceedings of IEEE Global Telecommunications Conference*, Nov. 2004.
- [25] —, "Limited feedback diversity techniques for correlated channels," *IEEE Transactions on Vehicular Technology*, vol. 55, no. 2, pp. 718–722, Mar. 2006.
- [26] P. Xia and B. G. Georgios, "Design and analysis of transmit-beamforming based on limited-rate feedback," *IEEE Transactions on Signal Processing*, vol. 54, no. 5, pp. 1853–1863, May 2006.
- [27] V. Raghavan, A. M. Sayeed, and V. V. Veeravalli, "Limited feedback precoder design for spatially correlated MIMO channels," in *Proceedings of Conference on Information Sciences and Systems*, Mar. 2007.
- [28] V. Raghavan, J. Choi, and D. J. Love, "Design guidelines for limited feedback in the spatially correlated broadcast channel," *IEEE Transactions on Communications*, vol. 63, no. 7, pp. 2524–2540, Jul. 2015.
- [29] *Study on 3D channel model for LTE*, 3GPP TR 36.873 V12.0.0 Std., Sep. 2014.
- [30] *Spatial channel model for multiple input multiple output simulations*, 3GPP TR 25.996 V6.1.0 Std., Sep. 2003.
- [31] R1-103378, *Performance evaluations of Rel.10 feedback framework*, 3GPP TSG RAN WG1 #61 Std., May 2010.
- [32] R1-105011, *Way forward on 8Tx codebook for Rel.10 DL MIMO*, 3GPP TSG RAN WG1 #61 Std., Aug. 2010.
- [33] Y. Han, S. Jin, X. Li, Y. Huang, L. Jiang, and G. Wang, "Design of double codebook based on 3D dual-polarized channel for multiuser MIMO system," *EURASIP Journal on Advances in Signal Processing*, vol. 2014, no. 1, pp. 1–13, Jul. 2014.
- [34] R. J. Mailloux, *Phased array antenna handbook*, 2nd ed. Artech House, 2005.
- [35] D. Ying, F. W. Vook, T. Thomas, D. J. Love, and A. Ghosh, "Kronecker product correlation model and limited feedback codebook design in a 3D channel model," in *Proceedings of IEEE International Conference on Communications*, Jun. 2014.
- [36] O. E. Ayach, S. Rajagopal, S. Abu-Surra, Z. Pi, and R. W. Heath, "Spatially sparse precoding in millimeter wave MIMO systems," *IEEE Transactions on Wireless Communications*, vol. 13, no. 3, pp. 1499–1513, Mar. 2014.
- [37] M. Borga, "Learning multidimensional signal processing," Ph.D. dissertation, Linköping University, Linköping, Sweden, 1998, SE-581 83.
- [38] A. Stuart and K. Ord, *Kendall's advanced theory of statistics: distribution theory*, 6th ed. London: Arnold, 1998.
- [39] H. David, *Order statistics*, 2nd ed. New York: John Wiley and Sons, 1980.